

Reviewer's comments in black, replies in blue.

Comments from Reviewer 1:

This paper provides a valuable contribution since there is not a huge amount of updraft information of this type in the literature. The results are valuable for a variety of reasons such as for providing better realism for numerical models on convection vertical motion scales and magnitudes. The results are also very useful for microphysical studies such as rain/snow growth mechanisms that require a vertical motions as a key input. The authors provide a good summary of past work and the manuscript in general is well written except for numerous typographical errors and some poorly worded sentences. The technical details are sufficient for the material presented. There is too much detail in some sections, and only the key points should be included (e.g., section 4.3).

Answer:

We appreciate the reviewer's comment. Actually, the Editor had pointed out the typographical errors after we submitted the original manuscript, then we sent the manuscript out for editorial service and submitted a revised version. However, when dealing with the technical comments, we found many typographical errors do exist in the old version, but have been corrected in the revised version. Maybe the reviewers were reading the old version. The revised version can be downloaded on <http://www.atmos-chem-phys-discuss.net/acp-2015-1021/#discussion> . Nevertheless, the sciences are the same. We have addressed the comments

raised by the reviewer, the sample issue and limitations of aircraft measurements have been highlighted. Sections with too much detail are simplified. A discussion section has been added to show the complicated interactions among vertical velocity, entrainment/detrainment and microphysics. We have changed the manuscript title to “Characteristics of Vertical Air Motion in Isolated Convective Clouds” to highlight that this study deals with isolated convections rather than mesoscale convective systems.

The paper deals with what shallow to moderate convection. The authors need to add some discussion in the abstract and conclusions on the fact that the measurements presented are still a biased sample of convection. Are the measurements truly representative of all convection in the three regions presented, or did for example the planes used stay away from stronger, and/or deeper convection, or ones with higher reflectivity. What the paper points out is that there are some similarities between the regions, but that there is really a wide variety of convective types over the globe. This is a good point to make in the paper that there are few measurements of this sort so they are greatly needed, but they represent specific regions and types of convection, more from other regions are needed, and one should not interpret the results that these results can be generalized globally. A few summary sentences (abstract, intro, and conclusions) on this point would make the paper better.

Answer:

We appreciate the comment. We totally agree that this study only deals with a biased sample of convective clouds. Only three field campaigns are analyzed and MCSs were not sampled. The

results cannot be generalized globally. We have pointed this out in the revised manuscript, included in abstract, introduction, datasets description and conclusion. We also changed the manuscript title to “Characteristics of Vertical Air Motion in Isolated Convective Clouds” to highlight that this study deals with isolated convections rather than mesoscale convective systems.

In addition, we have added more text to point out the limitations of aircraft measurements. First, aircraft cannot provide 3-D information of the cloud, so the air mass flux is derived from measurements in single-line penetrations. Second, aircraft might not penetrate through the strongest part of drafts due to safety issues. Moreover, in-situ measurements only provide data from single-line penetrations, but the vertical velocities are very different at different heights in a cloud. For example, many penetrations in COPE are near cloud top, while in HiCu and ICE-T there are many penetrations far below cloud top. Therefore, readers need to be aware of the limitations of aircraft measurements when using the results in this study.

While I find the paper quite interesting, there could be more connection between the convection dynamics and microphysics. Processes such as mixing are barely mentioned in the text. It would be interesting for example to make connections between the updraft characteristics such as mass fluxes, diameters, and entrainment.

Answer:

We appreciate the comment. We have tried to explore the interactions between dynamics and microphysics, but the physical processes are very complicated and there are many limitations

of aircraft instruments (e.g. resolution, time response and uncertainty) and sample issues. An example is given in Fig. R1. In the figure, we plot the mean vertical velocity (a and b), normalized relative humidity (c and d), normalized FSSP concentration and normalized King LWC (e and f) as a function of normalized scale from cloud edge to location of the maximum vertical velocity in the updraft closest to the cloud edge. On the x-axis, 0 indicates the cloud edge, 1 indicates the location of maximum vertical velocity in the updraft closest to the cloud edge, where is less affected by entrainment. As shown in the figure, weaker updraft associates with lower relative humidity, droplet concentration and LWC, and stronger updraft associates with higher relative humidity, droplet concentration and LWC. This maybe partly due to entrainment/detrainment mixing. This figure is from ICE-T only because in HiCu and COPE we do not have fast-response instrument to measure RH. The droplet concentration and LWC may have large uncertainty because FSSP often has shattering issues and King probe cannot detect large drops ($> 50\mu\text{m}$).

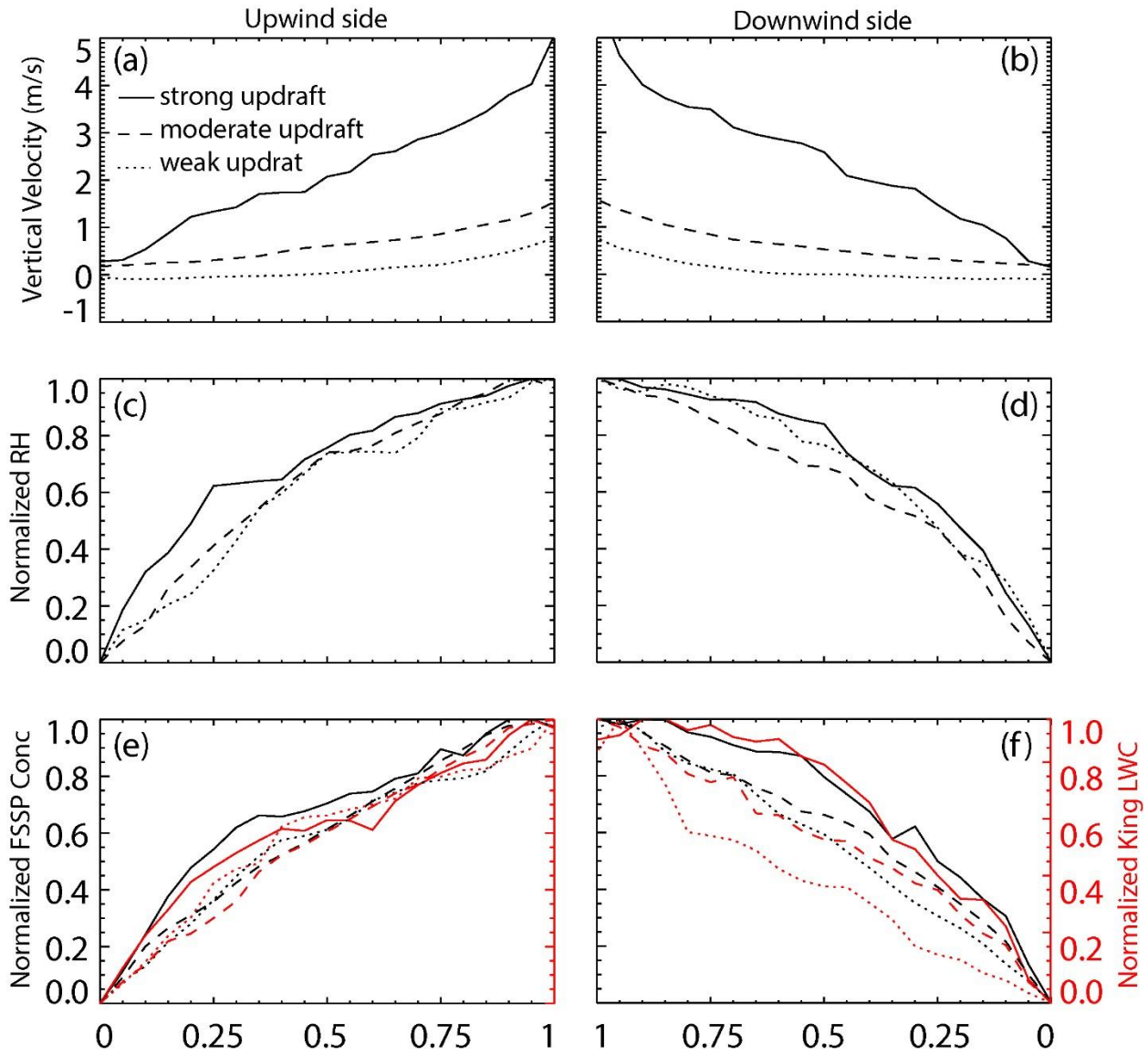


Fig. R1: Mean vertical velocity (a and b), normalized relative humidity (c and d), normalized FSSP concentration and normalized King LWC (e and f) as a function of normalized scale from cloud edge to updraft closest to the edge. 0 on the x-axis indicates the cloud edge, 1 on the x-axis indicates the location of maximum vertical velocity in the updraft closest to the cloud edge.

We also tried to use indirect ways to explore the impacts of entrainment on vertical velocity. Fig. R2 shows the PDF of vertical velocity in downdrafts near cloud edge and inside cloud. In HiCu and COPE the downdrafts near cloud edge are stronger than those inside clouds, maybe because of the strong evaporation-cooling effect induced by entrainment, while in ICE-T the downdrafts are similar near cloud edge and inside cloud. This only partly explains the stronger downdraft in HiCu and COPE than ICE-T, because the downdrafts inside clouds are also stronger in HiCu and COPE than ICE-T.

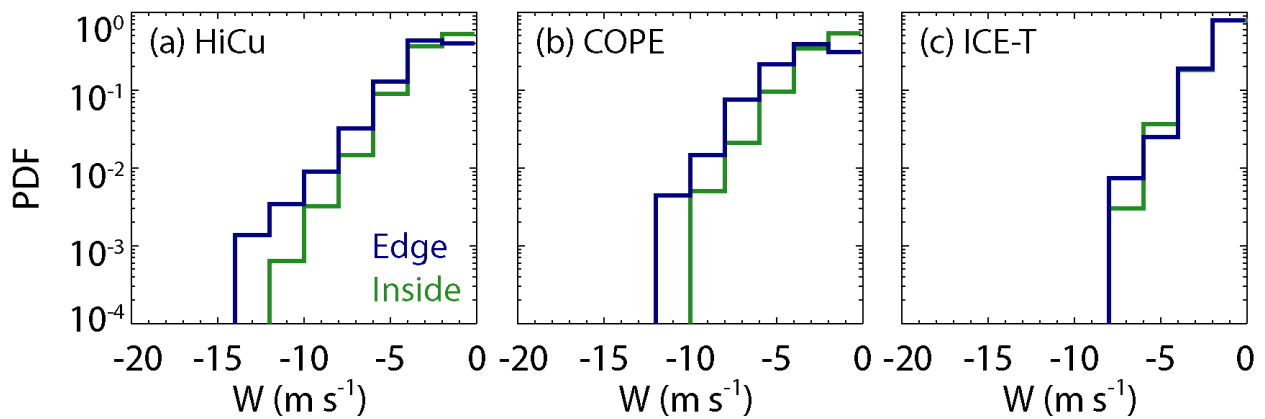


Fig. R2: PDFs of vertical velocity in downdrafts near cloud edge and inside cloud.

Due to the complexity of dynamics-microphysics interactions and the limitations of aircraft measurements, it is better to address this problem in detail in other papers. We have written a separated paper and discussed the interaction between vertical velocity and liquid-ice mass partitioning (Yang et al. manuscript submitted to JAS), in which an algorithms is developed to partitioning liquid and ice mass using multiple in-situ instruments. An example is given in Fig. R3, the figure shows in developing cloud the LWC and IWC are higher in stronger updraft, but

the liquid fraction has no obvious correlation with vertical velocity. In mature clouds, LWC is higher in stronger updrafts, but IWC is similar in weak and strong updrafts. Between -3 C and -8 C, the liquid fraction is smaller in weaker updrafts, maybe because secondary ice production (e.g. H-M process) is more significant in weaker updraft (Heymsfield and Willis 2014). Only ICE-T is used in that paper because in COPE and HiCu we do not have the appropriate instruments to provide sufficient measurements.

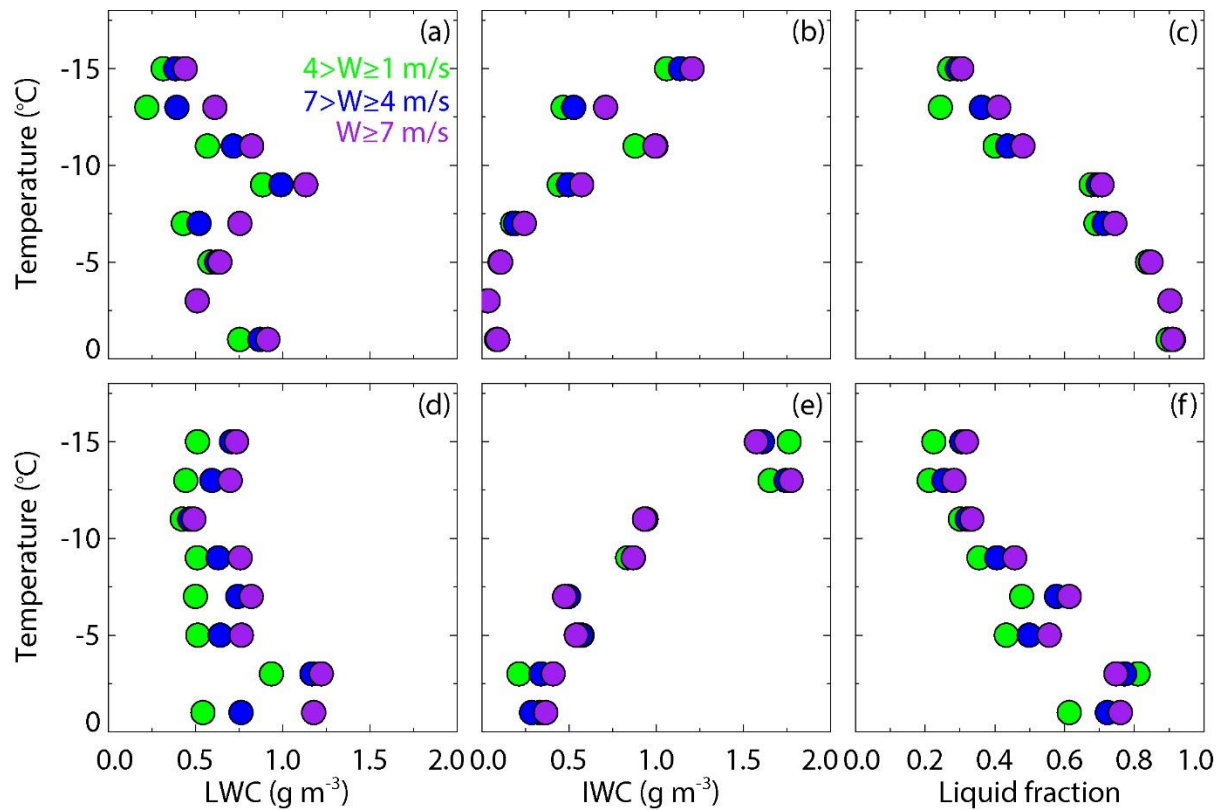


Fig. R3: The mean profiles of LWC, the IWC, and the liquid fraction as a function of temperature for the (a-c) young turrets and (d-f) mature turrets with vertical velocities of 1 m s⁻¹ – 4 m s⁻¹ (green), 4 m s⁻¹ – 7 m s⁻¹ (blue) and greater than 7 m s⁻¹ (purple).

In the revised manuscript, we decide to add a discussion section to highlight the importance of the interactions between dynamics and microphysics, and discuss the possible impacts of entrainment and microphysics on vertical velocity.

Technical and other details:

Lines 128-138: What are typical reflectivity in the convection. I know this will be from the W-band radar but this information would still be useful.

Answer:

The reflectivity depends on the stage of the clouds. The reflectivity in convective core is typically 10-20 dBZ in ICE-T, 5-20 dBZ in COPE, and 0-15 dBZ in HiCu. These reflectivity values may not reveal the maximum reflectivity in convective cores due to sampling issue. We've added this information in the text.

Lines 171: Define strong updrafts since these are still relatively weak compared to deeper convection.

Answer: We have changed “strong updrafts” to “relatively strong updrafts”. And have added *“These drafts maybe strong for isolated convections, but not necessary strong compared to MSCs”*.

Line 189: This accuracy (0.2 m/s) is quite good. Is there any chance there are biases rather than random errors on the vertical velocity?

Answer: There are no other instruments as references to provide systematic errors on vertical velocity. In the three datasets we do not see unrealistic values of vertical velocity (except a few cases in which the instrument was not working, which have been excluded in the study). Generally, the 0.2 m/s could be seen as the systematic error, random error could be larger than 0.2 m/s.

Line 209: Footnote. This is roughly the sensitivity of CloudSat. Is this the reason -30 dBZ was chosen since there will be cloud at lower reflectivities?

Answer: We choose this threshold by plotting the reflectivity near flight level in cloud free air. As shown in Fig. 2 in the manuscript, the reflectivity near flight levels is about -30 dBZ in cloud free air due to WCR signal noise. At levels far above or below flight level, the noise level is higher. In this study we mainly use in-situ measurement, so we only consider the reflectivity near flight level. Clouds with reflectivity lower than the noise level cannot be identified by WCR, and are excluded in this study, most of them maybe not convective clouds.

Lines 233-235: How do you know the 2D symmetry of the updraft since you might not fly through the peak up and downdrafts? Both the W-band radar and in situ measurements will not tell you this.

Answer: Here we want to show whirling penetrations and penetrations with significant turns have been rejected, so the cloud scale will not be significantly overestimated. We have modified this sentence to make it clear.

Line 236: “there is no” should be “there are no”

Answer: The comment has been addressed in the revised manuscript.

Line 238: Excluding MCS biases the results. This comes down to emphasis in this paper on small to moderate convection rather than deep convection in MCSs. Might mention this to keep the scope of your study in perspective.

Answer: We have pointed out the sample issue in the revised manuscript, including abstract, introduction, datasets description and conclusion. We also changed the manuscript title to “Characteristics of Vertical Air Motion in Isolated Convective Clouds” to highlight that this study deals with isolated convections rather than mesoscale convective systems.

Figure 4: need labels for field experiment associated with each color.

Answer: Labels have been added.

Lines 264-268: It might be useful to plot one example of a trace through one of the updraft/downdraft penetrations. This would be helpful to understand some of the averaging performed.

Answer:

Good suggestion. But the clouds were randomly sampled in the three field campaigns, we do not have continuous penetrations in one updraft/downdraft. More data are needed in the future. In addition, in-situ data itself is not enough to resolve the fine structure, in Fig. 2 in the manuscript, we can see many fine structures from the Doppler velocity measured by WCR, in-situ measurements can capture the details at single levels.

Line 268: “turbulences” to “turbulence”

Answer: “turbulences” has been changed to “turbulence” in the revised manuscript.

Line 300: “convections” to “convection”

Answer: “convections” has been changed to “convection” in the revised manuscript.

Line 294: “strong draft” – I would again put this in perspective since it is strong in your study, but not necessarily strong with respect to MCS updrafts for example.

Answer: We have add a sentence to indicate the definition of “strong” is only for this study, but not necessarily strong with respect to other convections (e.g. MCS): *“The definition of “weak”, “moderate” and “strong” only apply for this study. Other convections (e.g. MCS) could have much stronger updrafts.”*

Line 323-324: Again, this point should be more prominent in the paper.

Answer: We have highlighted that the definition of “weak”, “moderate” and “strong” only apply for this study.

Lines 386-387: This statement should be in the summary/conclusions since these measurements are important but we need a lot more.

Answer: We have added this statement in the conclusion.

Line 397: “results” to “result”

Answer: “results” has been changed to “result” in the revised manuscript.

Line 403: “relatively” to “relative”

Answer: “relatively” has been changed to “relative” in the revised manuscript.

Figure 10 and similar plots: I find these plots a little complicated and confusing but probably acceptable for publication. I can’t think of an alternative but possibly there is a better way to plot.

Answer: We tried to improve the figures but haven’t found a better way, because there are a lot of information in the figure. We have modified the text to better describe this figure.

Line 422: Some of the statements in this section should go in a summary and conclusions section. Points like lines 468-473 are important summary statements. You should consider pulling some of the summary points like this and putting them in the conclusions.

Answer: Statements with key points have been added in the conclusion.

Line 469: “pervious” to “previous”

Answer: “pervious” has been changed to “previous” in the revised manuscript.

Lines 509-510: “While in this study” should be something like “In contrast, this study shows the strongest. . .”

Answer: The sentence has been changed to *“In contrast, this study shows the strongest updrafts and downdrafts were observed at higher levels”*.

Line 522: “When exclude” to “When we exclude” Line 536: “convective cloud” to “convective clouds”

Answer: The comment has been addressed in the revised manuscript.

Lines 539-540: Can you say anything about the two-dimensionality of drafts from the remote sensing data?

Answer: We have added the following sentence in the text: “for example, airborne radar with slant and zenith/nadir viewing beams can provide two-dimensional wind structure in convective clouds”.

Line 553: “with expectation” to “expected”

Answer: “with expectation” has been changed to “expected” in the revised manuscript.

Line 564: “Since . . .to better”. This is an obvious fact. May want to just say that the aircraft just provides a line of data through drafts, and not vertical information unless the plane makes multiple passes through the same cell.

Answer: We have changed to sentence to “Since the aircraft just provides a line of data through drafts, and not vertical information unless the plane makes multiple passes through the same cell, more data, including remote sensing measurements are needed to better understand the evolution of the vertical velocity in convective clouds at different stages.”

Line 568: in the Summary section, you should reiterate the criteria for considering up/downdrafts, i.e., >xx m/s.

Answer: The criteria for considering up/downdrafts is reiterated.

Line 596: Flux calculations assume two-dimensionality of drafts and this might not be the case. Should mention this as a weakness in the study, i.e., using a single line penetration through drafts to make flux calculations.

Answer: We have highlighted that due to the limitation of aircraft measurements, the air mass flux is calculated using the data from single line penetrations. This may not fully capture the real air mass flux in the clouds and is a weakness of this study.

Comments from Reviewer 2:

I always like to see an in-depth study of vertical motions in the atmosphere because, as the authors point out, understanding these is vital to improving our understanding of (and hence modeling capabilities) many processes influenced by vertical motions. First, before I get to the science, this document was not ready for submission in any form. It is riddled with typographical errors making it very difficult to get to the science. I started to list them but, frankly, this is the job of an editorial service, something I recommend the author take advantage of. For example: "The COPE project was conducted from 03 July to 21 August, 2013". This is not English.. "The COPE project was conducted from the 3rd of July to the 21st August, 2013".. Write in English not in code. I have two broad areas of concern with this manuscript:

Answer:

We appreciate the reviewer's comment and sorry for the typographical errors. Actually, the Editor had pointed out the typographical errors after we submitted the original manuscript, then we sent the manuscript out for editorial service and submitted a revised version. However, when dealing with the technical comments raised by Reviewer 1, we found that many typographical errors pointed out by the Reviewer 1 exist in the old version, but have been corrected in the revised version. Maybe the reviewers were reading the old version. The revised version can be downloaded on <http://www.atmos-chem-phys-discuss.net/acp-2015-1021/#discussion> . In this round of revision, we have corrected a few more typographical errors.

I have two broad areas of concern with this manuscript:

1) The authors do not address the idea of sample size or sample bias OR more importantly geometric issues of sampling, in a line, a 2/3D object (being an updraft core). See Giangrande et al 2013 for a discussion of issues with profiler systems and angle of attack. Basically if you dissect an updraft core how do you know if you hit the strongest part of the updraft? Furthermore, up until the end, the idea of selection bias is not addressed. Even the C-130 will avoid the strongest cores. You can not build a PDF out to the tail from aircraft measurements. You can, as the paper did somewhat, look at intrinsic updraft properties. But you can not look at the distribution. I am somewhat disappointed, given the brief reference to microphysical measurements, that the authors did not relate vertical motions to microphysical properties of the updraft cores. This is something in-situ platforms are uniquely capable of doing. Also, in the literature review of methodologies for measuring vertical motions the authors neglect scanning radar measurements such as those shown in Collis et al 2013 and Nicol et al 2015 (not to mention a raft of airborne radar measurements from the NOAA p3 (look for papers from Jorgensen) and other aircraft that use the vertical plus 45 degree tilt methods.

Answer:

We totally agree with the reviewer that there are many limitations in aircraft measurements. First, aircraft might not penetrate through the strongest part of drafts due to safety issues. In addition, aircraft cannot provide 3-D information of the cloud, and the air mass flux is derived from measurements in single-line penetrations. Moreover, this study only deals with isolated convective clouds. Only three field campaigns are analyzed and MCSs are excluded in this study. The results cannot be generalized globally. We have pointed out these weaknesses in the revised

manuscript, including abstract, introduction, datasets description and conclusion. We also changed the manuscript title to “Characteristics of Vertical Air Motion in Isolated Convective Clouds” to highlight that this study deals with isolated convections rather than mesoscale convective systems (MCSs).

For the PDF distributions, we think it will be good to keep them the paper even though there are potential sampling issues. First, modelers do need the aircraft measurements to provide PDF distributions of vertical velocities (personal communications: Guangjun Zhang, Xiaohong Liu and Sungsu Park). Second, due to the relative small sizes of isolated convective clouds, the sampling bias associated with where to penetrate clouds is not as large as sampling MCSs. During the sampling of isolated convective clouds, we typically aligned the central part of cloud to penetrate at the flight height. During ICE-T and COPE, we have penetrations in updrafts stronger than 20 m/s (please note this is just for isolated convections, in which the updrafts are weaker than MCSs), and previous studies based on in-situ data rarely reported such relatively strong updrafts. Actually, this is one of our motivations to make this study. The PDFs can also be used to evaluate and improve remote sensing retrievals because in-situ measurements are more accurate than remote sensing, especially in mixed-phase convective clouds. Then remote sensing can provide PDFs out to the tail. Therefore, the PDFs in the paper still provide valuable information, but readers do need to be aware of the weaknesses and limitations of aircraft measurements.

We tried to explore the interactions between microphysics and vertical velocity, but the physical processes are very complicated, and there are many limitation of aircraft instruments in measuring the microphysics in mixed-phase convective clouds. For example, FSSP has the

shattering issue, hot-wire probes often underestimate the LWC because there are many large drops which cannot be directly sampled by these probes. Due to the complexity of dynamics-microphysics interactions and the limitations of aircraft measurements, it is better to address this problem in detail in other papers. We have written a separated paper and discussed the interaction between vertical velocity and liquid-ice mass partition in the mixed-phase cloud region within convective clouds (Yang et al. manuscript submitted to JAS), in which an algorithms is developed to partitioning liquid and ice mass using multiple in-situ instruments. An example is given in Fig. R3 (please find Fig. R3 in the response to Reviewer 1), the figure shows in developing cloud the LWC and IWC are higher in stronger updraft, but the liquid fraction has no obvious correlation with vertical velocity. In mature clouds, LWC is higher in stronger updrafts, but IWC is similar in weak and strong updrafts. Between -3 C and -8 C, the liquid fraction is smaller in weaker updrafts, maybe because secondary ice production is more significant in weaker updraft (Heymsfield and Willis 2014), results in relatively larger fraction of IWC. Such in-depth analyses only can be applied to ICE-T measurements in that paper because in COPE and HiCu we do not have the appropriate instruments to provide sufficient measurements.

Other than the interactions between vertical velocity and microphysics, entrainment/detrainment mixing also have impact on vertical velocity. But due to the complexity of the physical processes and the limitations of aircraft instruments, we think it is better to address this problem in detail in separated paper as well. (Please see the reply to Reviewer 1's comments).

In the revised manuscript, we add a discussion section to highlight the importance of the interactions between dynamics and microphysics, and discuss the possible impacts of entrainment and microphysics on vertical velocity.

In the revised manuscript, we have added the literatures about ground-based and airborne volumetric radar measurements in Introduction. For example, "*Collis et al. (2013) provides statistics of updraft velocities for difference convective cases near Darwin, Australia using retrievals from ground-based scanning Doppler radars and a multifrequency profiler*". "*Airborne volumetric Doppler radars have also been used to study the dynamic structure of convective clouds (e.g. Jorgensen and Smull 1993; Hildebrand et al. 1996; Jorgensen et al. 2000)*". "*Remote sensing has the advantage of being able to measure the vertically velocity at different heights simultaneously (Tonttila et al., 2011), and some of the techniques can detect the strongest updraft cores in convective clouds (Heymsfield et al. 2010; Collis et al. 2013)*". "*Volumetric radars can provide three-dimensional (3D) structure of air motion in convective clouds (Collis et al. 2013; Nicol et al. 2015; Jorgensen et al. 2000)*".

2) This comment relates to a specific question asked by the Journal in its review criteria "Are substantial conclusions reached?". I am deeply concerned by the authors attempt to relate the three field programs and say something about maritime versus continental convection. For one, the author did not put the cases into context. What was the CAPE for various cases? etc.. A selection of clouds at each campaign a climatology does not make. While the author caveats his comparison even the attempt to contrast the different regime is dangerous. For one, as mentioned, the strongest cores in the region of HiCu would all but destroy even the C-130 (See the various

photos associated with the Byers et al study of hail damage). To attempt to make a comparison, then state it goes contrary to common conception (Continental » Maritime) and then turn around and say "we did not sample the strongest updrafts in the continental case" is disingenuous.

So negatives out of the way, one of the things that redeem the paper is the focus on updraft shape and how that varies with height. Personally I find this very interesting as not only does the mass flux of a plume influence transport but the vertical velocity within determines many microphysical aspects. ie a plume that starts thin and then expand for the same mass flux would have lower vertical velocities aloft influencing processes like Hallett-Mossop splintering etc.. (and associated latent feedbacks).. The paper should focus more on this and the *intrinsic* differences. Things that are co-varying and less susceptible to sampling and decision bias.

Answer:

We appreciate the reviewer's comments. We have pointed out the weaknesses of aircraft measurements in the revised manuscript, including abstract, introduction, datasets description and conclusion, as well as the title.

Due to the limitation of aircraft measurement, we have deleted some results which are sensitive to the sampling issue. For example, "the vertical velocity in HiCu is weaker than that in COPE and ICE-T". In addition, in this paper we plot the vertical velocity PDFs and profiles as a function of height MSL (Fig. 8 and 10), so at the same height, the vertical velocity maybe weaker in HiCu. However, the updrafts were strengthening with height, and some updrafts could be close to 20 m/s at > 6 km MSL (Fig. 8) in HiCu. Maybe at higher levels the updrafts in HiCu were stronger than COPE and ICE-T, but we do not have more data. If we plot the updraft PDFs

and profiles as a function of height above cloud base, the results in HiCu maybe closer to that in COPE and ICE-T. However, cloud base heights are variable and we do not have data to calculate the cloud base heights.

In the revised paper, we have added some text to describe the ambient conditions which many affect the vertical air motion. For example, *“the convective available potential energy (CAPE) in ICE-T is greater than 2000 J kg⁻¹. The CAPE in COPE is typically a few hundred J kg⁻¹. No soundings are available for HiCu, so we have to use aircraft measurements to estimate the CAPE. In some cases, the full CAPE cannot be calculated since the aircraft only flew at low levels (< 10 km MSL). The aircraft measurements suggest the CAPE in HiCu ranges from less than 100 J kg⁻¹ to more than 500 J kg⁻¹”*.

As suggested by the reviewer, we have added more discussion about the *intrinsic* differences among the three field campaigns. For example, the downdrafts in HiCu and COPE are obviously stronger than that in ICE-T, maybe partly due to the evaporation-cooling effect induced by entrainment (please see the reply to Reviewer 1). We also changed Fig. 11 to Fig. R2 as follows to show how the draft shape changes with height. Actually, the evolution of draft with height is very complicated. Based on our datasets, there could be different possibilities: 1) an updraft expands and the vertical velocity weakens with height, 2) an updraft expands and the vertical velocity strengthens with height, 3) an updraft splits to multiple updrafts and downdrafts, 4) two updrafts merged and become one updrafts. Since we do not have continuous penetrations in a single cloud, we have to statistically analyze the evolution of draft shape. In Fig. R4, we can see that the normalized shape do not have significantly change with height, the peak vertical velocity is strengthening with height. Connecting this figure to diameter (Fig. 4), vertical

velocity (Fig. 8) and air mass flux (Fig. 9), the results show statistically, the drafts were expanding (Fig. 4) and the vertical velocity was strengthening (Fig. R2 and 8), but the air mass flux was not increasing (Fig. 9). This reveals the complicated physical processes (e.g. entrainment, water loading and the possibilities described above). The interaction between vertical velocity evolution and microphysics is even more complicated and needs to be analyzed in detail in separated papers (please see the reply to the first comment above).

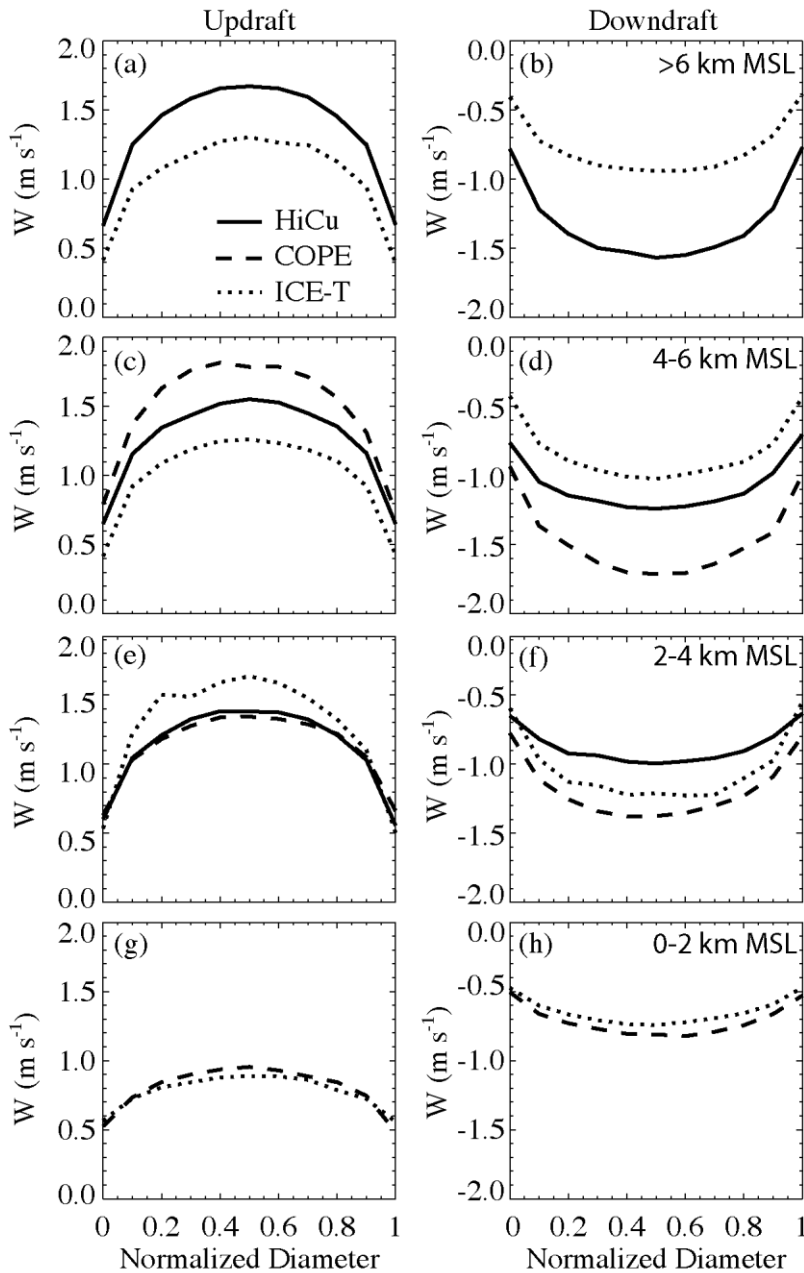


Fig. R4: Composite structure of the vertical velocity as a function of the normalized diameter for the updrafts and downdrafts with air mass flux $\geq 10 \text{ kg m}^{-1} \text{ s}^{-1}$ in magnitude. The 0 and 1 coordinates on the x-axis indicate the upwind and downwind sides of the draft.

Finally, we want to say this paper is just a part of the whole picture. The physical processes in mixed-phase convective clouds (e.g. interaction between dynamics and microphysics) are very complicated, and need to be further explored in the future with more experimental data, especially with more advanced measurements. The contributions of this paper are 1) provides

statistical results of vertical air motion in isolated convective clouds using in-situ data in recent field campaigns, which could be used to evaluate remote sensing retrievals and model simulations. 2) In-situ measurements of vertical velocity stronger than 20 m/s in isolated convective clouds are provided. Previous studies using in-situ measurement rarely had penetrations in such relatively strong updrafts. 3) This paper highlights the importance of small drafts using high-resolution in-situ data, which is not shown in previous studies. 4) Some ‘intrinsic’ differences and similarities of vertical air motions among the three field campaigns are discussed. Aircraft measurements do have many limitations and this paper only deals with isolated convections, we have highlighted them in the revised paper.

1 Characteristics of Vertical Air Motion in Isolated Convective

2 Clouds

3
4 **Jing Yang¹, Zhien Wang¹, Andrew J. Heymsfield² and Jeffrey R. French¹**

5 [1] {Department of Atmospheric Science, University of Wyoming, Laramie, WY}

6 [2] {National Center for Atmospheric Research, Boulder, CO}

7 Correspondence to: Zhien Wang (zwang@uwyo.edu)

8 9 **Abstract**

10 The vertical velocity and air mass flux in isolated convective clouds are statistically analyzed
11 using aircraft in-situ data collected from three field campaigns: High-Plains Cumulus (HiCu)
12 conducted over the mid-latitude High Plains, CONvective Precipitation Experiment (COPE)
13 conducted in a mid-latitude coastal area, and Ice in Clouds Experiment-Tropical (ICE-T),
14 conducted over a tropical ocean. This study yields the following results. (1) Small-scale updrafts
15 and downdrafts (< 500 m in diameter) are frequently observed in the three field campaigns, and
16 they make important contributions to the total air mass flux. (2) The probability density functions
17 (PDFs) and profiles of the vertical velocity are provided. The PDFs are exponentially distributed.
18 The updrafts generally strengthen with height. Relatively strong updrafts (> 20 m s⁻¹) were
19 sampled in COPE and ICE-T. ~~For updrafts, the PDFs of the vertical velocity are broader in ICE-~~

20 ~~T and COPE than in HiCu; for downdrafts, the PDFs of the vertical velocity are broader in HiCu~~
21 ~~and COPE than in ICE-T. (3) Vertical velocity profiles show that updrafts are stronger in ICE-T~~
22 ~~and COPE than in HiCu, and~~ The downdrafts are stronger in HiCu and COPE than in ICE-T. (4)
23 The PDFs of the air mass flux are exponentially distributed as well. The maximum air mass flux
24 in updrafts is of the order $10^4 \text{ kg m}^{-1} \text{ s}^{-1}$. The air mass flux in the downdrafts is typically a few
25 times smaller in magnitude than that in the updrafts. Since this study only deals with a biased
26 sample of isolated convective clouds, and there are many limitations and sampling issues in
27 aircraft in-situ measurements, more observations and simulations are needed to better explore the
28 vertical air motion in convective clouds.

29

30 **1. Introduction**

31 Convective clouds are an important component of the global energy balance and water cycle
32 because they dynamically couple the planetary boundary layer to the free troposphere through
33 vertical heat, moisture and mass transport (Arakawa, 2004; Heymsfield et al., 2010; Wang and
34 Geerts, 2013). The vertical velocity determines the vertical transport of cloud condensate, the
35 cloud top height and the detrainment into anvils, which further impact the radiative balance (Del
36 Genio et al., 2005). Vertical velocity also has significant impact on the aerosol activation, droplet
37 condensation and ice nucleation in convective clouds, which control the cloud life cycle and
38 precipitation efficiency.

39 In order to reasonably simulate convective clouds, the vertical air velocity must be parameterized
40 reliably in numerical weather prediction models (NWPMs) and global circulation models (GCMs)
41 (Donner et al., 2001; Tonttila et al., 2011; Wang and Zhang, 2014). However, the complexity of

42 the vertical velocity structure in convective clouds makes the parameterization non-
43 straightforward (Wang and Zhang, 2014). Observations show that in most of the convective
44 clouds the vertical velocity is highly variable, and consequently the detailed structure of
45 convection cannot be resolved in many models (Kollias et al., 2001; Tonttila et al., 2011).
46 Additionally, using the same parameterization of vertical velocity for different grid resolutions
47 may result in different cloud and precipitation properties (Khairoutdinov et al., 2009).
48 Furthermore, poorly parameterized vertical velocity may result in large uncertainties in the
49 microphysics; for instance, the cloud droplet concentration may be underestimated due to
50 unresolved vertical velocity (Ivanova and Leighton, 2008). Vertical velocity simulated by
51 models with horizontal resolutions down to a few hundred meters may be more realistic (e.g. Wu
52 et al., 2009), but more observations are needed to evaluate this suggestion.

53 Aircraft in-situ measurement has been the most reliable tool enabling us to understand the
54 vertical velocity in convective clouds and to develop the parameterizations for models. Early
55 studies (e.g. Byers and Braham, 1949; Schmeter, 1969) observed strong updrafts and downdrafts
56 in convective clouds; however, their results have a large uncertainty, because the aircrafts were
57 not equipped with inertial navigation systems (LeMone and Zipser, 1980). In 1974, the Global
58 Atmospheric Research Program (GARP) Atlantic Tropical Experiment (GATE) was conducted
59 off the west coast of Africa, focusing on tropical maritime convections (Houze, 1981). A series
60 of findings based on the aircraft data collected from the project was reported. For example, the
61 accumulated probability density functions (PDFs) of vertical velocity and diameter of the
62 convective cores are lognormal distributed. The updrafts and downdrafts in GATE (tropical
63 maritime clouds) were only one half to one third as strong as those observed in the Thunderstorm
64 Project (continental clouds) (LeMone and Zipser, 1980; Houze, 1981). These findings stimulated

65 later statistical studies of the vertical velocity in convective clouds. Jorgensen et al. (1985) found
66 that the accumulated PDFs of vertical velocity in intense hurricanes were also lognormal
67 distributed and the strength was similar to that in GATE, but the diameter of the convective
68 region was larger. Studies of the convective clouds over Taiwan (Jorgensen and LeMone, 1989)
69 and Australia (Lucas et al., 1994) showed a magnitude of vertical velocity similar to that in
70 GATE. Although the results from the Thunderstorm Project are suspect, the significantly
71 stronger drafts reveal the possible difference between continental and tropical maritime
72 convective clouds. Lucas et al. (1994) suggested that the water loading and entrainment strongly
73 reduce the strength of updrafts in maritime convections. However, this underestimation of the
74 updraft intensity may be also due to the sampling issues, e.g. penetrations were made outside the
75 strongest cores (Heymsfield et al., 2010).

76 There are a few more recent aircraft measurements (e.g. Igau et al, 1999; Anderson et al., 2005),
77 but the data are still inadequate to fully characterize the vertical velocity in convective clouds. In
78 most of these earlier papers, the defined draft or draft core required a diameter no smaller than
79 500 m; this threshold excluded many narrow drafts with strong vertical velocity and air mass
80 flux. In addition, the earlier studies used 1-Hz resolution data, which can resolve only the vertical
81 velocity structures larger than a few hundred meters, but the narrow drafts may be important to
82 the total air mass flux exchange and cloud evolution. Furthermore, previous aircraft observations
83 for continental convective clouds were based only on the Thunderstorm Project; thus, new data
84 are needed to study the difference between continental and maritime convections.

85 Remote sensing by means of, for example, wind profilers and radars is another technique which
86 has often been used in recent years for studying the vertical velocity in convective clouds (e.g.
87 Kollias et al., 2001; Hogan et al., 2009; [Giangrande et al., 2013](#); Schumacher et al., 2015). Using

88 profiler data, May and Rajopadhyaya (1999) analyzed the vertical velocity in deep convections
89 near Darwin, Australia. They observed that the updraft intensified with height and that the
90 maximum vertical velocity was greater than 15 m s^{-1} . Heymsfield et al. (2010) studied the
91 vertical velocity in deep convections using an airborne nadir-viewing radar. Strong updrafts were
92 observed over both continental and ocean areas, with the peak vertical velocity exceeding 15 m s^{-1}
93 in most of the cases and exceeding 30 m s^{-1} in a few cases. Zipser et al. (2006) used satellite
94 measurements to find the most intense thunderstorms around the world; they applied a threshold
95 updraft velocity greater than 25 m s^{-1} to identify intense convection. [Collis et al. \(2013\) provides](#)
96 [statistics of updraft velocities for different convective cases near Darwin, Australia using](#)
97 [retrievals from scanning Doppler radars and a multifrequency profiler. Airborne volumetric](#)
98 [Doppler radars have also been used to study the dynamic structure of convective clouds \(e.g.](#)
99 [Jorgensen and Smull 1993; Hildebrand et al. 1996; Jorgensen et al. 2000\). Remote sensing has](#)
100 [the advantage of being able to measure the vertically velocity at different heights simultaneously](#)
101 [\(Tonttila et al., 2011\), and some of the techniques can detect the strongest updraft core in](#)
102 [convective clouds \(Heymsfield et al. 2010; Collis et al. 2013\). Volumetric radars can also](#)
103 [provide three-dimensional structure of air motion in convective clouds \(Collis et al. 2013; Nicol](#)
104 [et al. 2015; Jorgensen et al. 2000\).](#) However, remote sensing measurements are not as accurate as
105 aircraft measurements, because many assumptions are needed to account for the contribution of
106 hydrometeor fall speed in the observed Doppler velocity in order to ultimately estimate air
107 velocity. In addition, ground-based radars can rarely provide good measurements over oceans,
108 and airborne cloud radars often suffer from the attenuation and non-Rayleigh scattering in
109 convective clouds. Therefore, in-situ measurements are still necessary in order to characterize the
110 dynamics in convective clouds and to develop parameterizations for models.

111 The present study provides aircraft data analysis of the updrafts and downdrafts in mid-latitude
112 continental, mid-latitude coastal and tropical maritime convective clouds using the fast-response
113 in-situ measurements collected from three field campaigns: the High-Plains Cumulus (HiCu), the
114 COncvective Precipitation Experiment (COPE) and the Ice in Clouds Experiment-Tropical (ICE-
115 T). All the clouds formed in isolation, but some of them merged as they evolved. Statistics of the
116 vertical velocity and air mass flux are provided. The Wyoming Cloud Radar (WCR), onboard the
117 aircraft, is used to identify the cloud top height, and high frequency (25-Hz) in-situ
118 measurements of vertical velocity are used to generate the statistics. [The major limitations of](#)
119 [aircraft in-situ measurements are the aircraft maybe not able to sample the strongest part of](#)
120 [convections due to safety concern, and it only provides the information of vertical air motion at](#)
121 [single levels. These weaknesses need to be kept in mind in the following analyses.](#) Section 2
122 describes the datasets and wind measuring systems. Section 3 presents the analysis method.
123 Section 4 shows the results. [Section 5 discusses the possible factors those interact with vertical](#)
124 [air motions](#), and conclusions are given in Section ~~5~~6.

125

126 **2. Dataset and instruments**

127 **2.1 Dataset**

128 The data used in the present study were collected from three field campaigns: HiCu, COPE and
129 ICE-T. Vigorous convective clouds were penetrated during the three field campaigns, including
130 mid-latitude continental, mid-latitude coastal, and tropical maritime convective clouds. These
131 penetrations provide good quality measurements for studying the microphysics and dynamics in
132 the convective clouds, as well as the interactions between the clouds and the ambient air. The

133 locations of the three field campaigns are shown in Fig. 1. Information regarding the penetrations
134 used in this study is summarized in Table 1.

135 The HiCu project was conducted mainly in Arizona and Wyoming (Fig. 1) from [the 18th of July](#)
136 [to the 05th of August, 2002,](#) and from [the 07th of July to the 31st of August, 2003](#) to investigate
137 the microphysics and dynamics in convective clouds over mid-latitude High Plains. The
138 University of Wyoming King Air (UWKA) was operated as the platform. In 2002 and 2003, 10
139 and 30 research flights were made, respectively. In this study, the 2002 HiCu and 2003 HiCu are
140 analyzed together because they were both conducted over the High Plains and the sample size of
141 2002 HiCu is relatively small. Fast-response in-situ instruments and the Wyoming Cloud Radar
142 (WCR, Wang et al., 2012) were operated during the field campaign to measure the ambient
143 environment, cloud dynamics and microphysics as well as two-dimensional (2D) cloud structure.
144 As shown in Table 1, penetrations in HiCu were made between 2 km and 10 km MSL. The
145 sample size is relatively good below 8 km and relatively small above 8 km. The aircraft flew
146 about 2000 km in clouds. In-situ measurements and WCR worked well in these flights; however,
147 the upward-pointing radar was operated in less than half of the research flights, and thus only a
148 sub-set of the cloud tops can be estimated. Fig. 2a(1–3) shows an example of the clouds sampled
149 in HiCu, including WCR reflectivity, Doppler velocity and 25-Hz in-situ measurement of the
150 vertical velocity. In HiCu, both developing and mature convective clouds were penetrated; some
151 penetrations were near cloud top, while most of them were more than 1 km below cloud top. [The](#)
152 [typical WCR reflectivity is 0-15 dBZ in the convective cores due to strong Mie scattering at the](#)
153 [WCR wavelength.](#) From the Doppler velocity and the in-situ vertical velocity, we can see that, in
154 both the developing and mature cloud, [relatively](#) strong updrafts and downdrafts were observed,
155 and multiple updrafts and downdrafts existed in the same cloud. [These drafts maybe strong for](#)

156 [isolated convections, but not necessary strong compared to the strongest updrafts in mesoscale](#)
157 [connective systems \(MCSs\)](#). No soundings are available to measure the ambient environment in
158 HiCu, so we have to use aircraft measurements to estimate the [convective available potential](#)
159 [energy \(CAPE\)](#). In some cases, the full CAPE cannot be calculated since the aircraft only flew at
160 low levels (< 10 km MSL). The aircraft measurements suggest the CAPE in HiCu ranges from
161 less than 100 J kg⁻¹ to more than 500 J kg⁻¹.

162 The COPE project was conducted from [the 03rd of July](#) to [the 21st of August](#), 2013 in Southwest
163 England (Fig. 1). The UWKA was used to study the microphysics and entrainment in mid-
164 latitude coastal convective clouds (Leon et al., 2015). Seventeen research flights were conducted;
165 penetrations focused on regions near cloud top, which is verified based on the radar reflectivity
166 from the onboard WCR. Since COPE was conducted in a coastal area, the convection initiation
167 mechanism is different from that over a purely continental or ocean area. In addition, although
168 the ambient air mainly came from the ocean, continental aerosols might be brought into clouds,
169 since many of the convective clouds formed within the boundary layer, which further affects the
170 microphysics and dynamics in the clouds. The measurements made in COPE include temperature,
171 vertical velocity, liquid water content, and particle concentration and size distributions. The
172 WCR provided excellent measurements of reflectivity and Doppler velocity. The downward
173 Wyoming Cloud Lidar (WCL) was operated to investigate the liquid (or ice) dominated clouds.
174 [The typical WCR reflectivity is 5-20 dBZ in the convective cores](#). Between 0 km and 6 km,
175 about 800 penetrations were made. Flight distance in cloud totaled about 1000 km. The sample
176 sizes are relatively good between 2 km and 6 km, but relatively small between 0 km and 2 km.
177 Examples of the penetrations are given in Fig. 2b(1–3). COPE has fewer penetrations than HiCu,
178 and most of the penetrations are near the cloud top. Fig. 2b(2) reveals relatively simple structures

179 of the updrafts and downdrafts in COPE compared to HiCu, but as shown by the 25-Hz in-situ
180 vertical velocity measurement in Fig. 2b(3), there are still many complicated fine structures in
181 the vertical velocity distribution. The typical CAPE estimated from soundings in COPE was a
182 few hundred J kg⁻¹.

183 The ICE-T project was conducted from ~~the 1st of July~~ July 1 to ~~the 30th of July~~ 30, 2011 near St.
184 Croix, U.S. Virgin Islands (Fig. 1), with state-of-the-art airborne in situ and remote sensing
185 instrumentations, with the aim of studying the role of ice generation in tropical maritime
186 convective clouds. The NSF/NCAR C-130 aircraft was used during ICE-T to penetrate
187 convective clouds over the Caribbean Sea. Thirteen C-130 research flights were conducted
188 during the field campaign, with vigorous convective clouds penetrated. In-situ measurements
189 from ICE-T include the liquid and total condensed water contents, temperatures, vertical
190 velocities, and cloud and precipitating particle concentrations and size distributions. The WCR
191 was operated on seven research flights to measure the 2D reflectivity and Doppler velocity fields.
192 The typical WCR reflectivity in the convective cores is 10-20 dBZ. The aircraft flew more than
193 1500 km in clouds, and more than 650 cloud penetrations were made between 0 km and 8 km.
194 The sample sizes are good except between 2 km and 4 km (Table 1). Examples of the
195 penetrations are shown in Fig. 2c(1-3). During ICE-T, clouds in different stages were penetrated,
196 including developing, mature and dissipating, some near cloud top and some considerably below
197 cloud top. ~~Relatively s~~Strong Updrafts up to 25 m s⁻¹ updrafts were observed ~~in the developing~~
198 ~~and mature clouds, but~~ the downdrafts in ICE-T are typically weaker than those in HiCu and
199 COPE. The vertical velocity structures are complicated, as confirmed by both the Doppler
200 velocity and the 25-Hz in-situ measurement. Weak updrafts and downdrafts were also observed

201 in the dissipating clouds. The typical CAPE in ICE-T was greater than 2000 J kg⁻¹, which is
202 larger than that in HiCu and COPE.

203 During the sampling of isolated convective clouds in the three field campaigns, we typically
204 aligned the central part of cloud to penetrate at the flight height, but still, the aircrafts might not
205 penetrate through the strongest part of convective core due to safety concern. ~~In all the three field~~
206 ~~campaigns~~In addition, aircraft in-situ measurements only provide the information of vertical air
207 motion at single levels. Moreover, the clouds sampled are isolated convective clouds, MCSs
208 were not sampled. ~~Therefore, the results cannot be generalized globally.~~ These limitations need
209 to be kept in mind in interpreting results from the following analysis. ~~In addition, the aircrafts~~
210 ~~might not penetrate through the strongest part of convective core due to safety concern, e during~~
211 ~~the sampling of isolated convective clouds, we typically aligned the central part of cloud to~~
212 ~~penetrate at the flight height, and they only provide data at single levels. So the statistic shown in~~
213 ~~this study is just a part of the complete picture.~~

215 2.2 Wind measuring system

216 On both C-130 and UWKA, A Radome Five-Hole Gust Probe is installed for three-dimensional
217 (3D) wind measurement. A Radome Five-Hole Gust Probe is an aircraft radome probe with five
218 pressure ports installed in a “cross” pattern. Relative wind components (e.g. true air speed and
219 flow angles) are sensed by a combination of differential pressure sensors attached to the five
220 holes (Wendisch and Brenguier, 2013). Detailed calculation of relative wind components is
221 described in Kroonenberg et al. (2008) and Wendisch and Brenguier (2013). The time response
222 and the accuracy of the pressure sensors is about 25 Hz and 0.1 mb. The 3D wind vectors can be

223 derived by taking out the aircraft motions from the relative wind measurement. On both C-130
224 and UWKA, the aircraft motion is monitored by a Honeywell ~~Laseref~~[LASEREF](#) SM Inertial
225 Reference System (IRS), with an accuracy of 0.15 m s^{-1} for vertical motion. Global Positioning
226 System (GPS) was applied to remove the drift errors in the IRS position in all the three field
227 campaigns (Khelif et al., 1998). The final vertical wind velocity product has an accuracy of about
228 $\pm 0.2 \text{ m s}^{-1}$, and a time response of 25 Hz. This uncertainty ($\pm 0.2 \text{ m s}^{-1}$) is a mean bias. For each
229 output, the uncertainty is related to the true air speed, aircraft pitch angle, roll angle and ambient
230 conditions. Therefore, the random error varies and could be larger than the mean bias. More
231 information about the wind measurement on C-130 and UWKA can be found on the C-130
232 Investigator Handbook (available on <https://www.eol.ucar.edu/content/c-130-investigator->
233 [handbook](#)) and UWKA Investigator Handbook (available on
234 http://www.atmos.uwyo.edu/uwka/users/KA_InstList.pdf)

235

236 **3. Analysis method**

237 **3.1 Identifying cloud using in-situ measurements**

238 The Particle Measuring Systems (PMS) Two-Dimensional Cloud (2D-C) Probe and the Forward
239 Scattering Spectrometer Probe (FSSP) are often used to characterize cloud microphysics (e.g.
240 Anderson et al., 2004), although different thresholds of 2D-C and FSSP concentrations are
241 usually used to identify the edge of a cloud. In this paper, we also use FSSP and 2D-C probes to
242 find the cloud edges. In order to find a reasonable threshold for identifying cloudy air, we first
243 use the WCR reflectivity to identify the clouds and the cloud-free atmosphere; for those regions
244 we then plot the particle concentrations measured by FSSP and 2D-C in order to determine the

245 reasonable thresholds, and we apply the thresholds of particle concentrations to all the research
246 flights without WCR.

247 To identify clouds using WCR, the six effective range gates nearest to the flight level (three
248 above and three below) are chosen in each beam. Any beam in which the minimum reflectivity at
249 the six gates exceeds ~~the noise level~~ [-30 dBZ](#)¹ is identified as in cloud.

250 Fig. 3 shows the occurrence distribution as a function of the particle concentrations measured by
251 FSSP versus the concentrations of the particles $\geq 50 \mu\text{m}$ in diameter measured by 2D-C in the
252 clouds identified by WCR reflectivity. From the figure, we can see that the FSSP concentration
253 ranges from 0.01 cm^{-3} to 1000 cm^{-3} , and the 2D-C concentration ranges from 0.1 L^{-1} to 10000 L^{-1} .
254 Generally, shallow clouds have relatively higher concentrations of small particles and lower
255 concentration of particles larger than $50 \mu\text{m}$. In deeper convective clouds, high concentrations
256 can be seen for both small and large particles. The FSSP concentrations in cloud-free air are
257 found to be 2 cm^{-3} at most, and the FSSP concentrations measured below the lifting condensation
258 level (LCL), where precipitating particles dominated, are lower than 2 cm^{-3} , as well. Therefore, 2
259 cm^{-3} is selected as the concentration threshold to identify clouds based on the FSSP
260 measurements, as shown by the dashed line in Fig. 3. However, in some clouds (e.g. pure ice
261 clouds), the FSSP concentration could be lower than 2 cm^{-3} , and 2D-C concentrations are needed
262 to identify these cold clouds. We chose a 1 L^{-1} 2D-C concentration for particles $\geq 50 \mu\text{m}$ as the
263 second threshold to identify cloud, as shown by the dotted line in Fig. 3. In order to avoid
264 precipitating regions (below the LCL calculated from soundings), the second threshold is only

¹ Based on the reflectivity measured in cloud-free air, the noise level of WCR reflectivity is -32 dBZ at a range of 500 m and -28 dBZ at a range of 1000 m . In this study, we choose -30 dBZ as the threshold to identify cloud. This threshold ([-30 dBZ](#)) is examined for all three field campaigns.

265 applied to penetrations at temperatures colder than 0 °C; thus the cloud is defined as FSSP
266 concentration $\geq 2 \text{ cm}^{-3}$ or 2D-C concentration $\geq 1 \text{ L}^{-1}$. At temperatures warmer than 0 °C, the
267 FSSP concentrations in most of the convective clouds are higher than 2 cm^{-3} , so only the first
268 threshold is used.

269 Once a cloud is identified, the penetration details can be calculated, including the flight length,
270 the flight height, the cloud top height if WCR is available, and the penetration diameter. The
271 penetration diameter is calculated as the distance between the entrance and exit of a penetration.

272 In order to reject whirling penetrations and penetrations with significant turns, we require that
273 the diameter of a penetration be at least 90% of the flight length. ~~so the cloud scale will not be~~
274 ~~significantly overestimated. The penetration diameter can generally reveal the scale of a cloud,~~
275 ~~but s~~Since the aircraft ~~may~~ might not penetrate exactly through the center of a cloud, the actual
276 cloud diameter may be larger than the penetration diameter. Based on WCR reflectivity images,
277 there are no isolated convective clouds sampled larger than 20 km in diameter. There are a few
278 penetrations longer than 20 km, but these clouds are more like ~~part of mesoscale convective~~
279 ~~systems (MCSs)~~, and so they are excluded from this study.

280

281 3.2 Defining updraft and downdraft

282 In previous studies of the vertical velocity based on in-situ measurements, the updraft and
283 downdraft are often defined as an ascending or subsiding air parcel with the vertical velocity
284 continuously $\geq 0 \text{ m s}^{-1}$ in magnitude and $\geq 500 \text{ m}$ in diameter (e.g. LeMone and Zipser, 1980;
285 Jorgensen and LeMone, 1989; Lucas et al., 1994; Igau et al., 1999). In this study, we use a
286 vertical velocity threshold of 0.2 m s^{-1} , that is, the draft has a vertical velocity continuously ≥ 0.2

287 m s⁻¹ in magnitude, because ±0.2 m s⁻¹ is the accuracy of the instrument. Any very narrow and
288 weak portion (diameter < 10 m and maximum vertical velocity < 0.2 m s⁻¹ in magnitude)
289 between two relatively strong portions is ignored, and the two strong portions are considered as
290 one draft.

291 The diameter threshold (500 m) is not used in this paper, because drafts narrower than 500 m
292 frequently occur and they make important contributions to the total air mass flux in the
293 atmosphere and therefore they are necessarily to be considered in model simulations. Fig. 4
294 shows the PDFs of the diameters of all the updrafts and downdrafts sampled in HiCu, COPE and
295 ICE-T. In all the panels, the diameters are exponentially distributed, the PDFs can be fitted using

$$296 \quad f = \alpha \cdot |x|^\beta \cdot \exp(\gamma|x|) \quad (1)$$

297 where f is the frequency and x is the diameter. The coefficients α , β and γ for each PDF is shown
298 in each panel. This function will also be used to fit the PDFs of vertical velocity and air mass
299 flux in the following analyses. Generally, as seen in Fig 4, the PDFs broaden with height
300 increases for the three field campaigns; this is consistent with previous findings (LeMone and
301 Zipser, 1980). The diameters of the updrafts are smaller in COPE compared to those sampled in
302 HiCu and ICE-T, possibly because most of the penetrations are near cloud top. ~~The diameters of
303 the downdrafts are relatively small in HiCu. ICE-T has the most drafts with diameters exceeding
304 100 m, and the average diameters in ICE-T for both updrafts and downdrafts are the largest.~~ As
305 shown in Fig. 4, many narrow drafts are observed. More than 85%, 90% and 74% of the updrafts
306 are narrower than 500 m (dotted lines) in HiCu, COPE and ICE-T, respectively, and more than
307 90% of the downdrafts in all three field campaigns are narrower than 500 m. A threshold of 500
308 m in diameter would exclude many small-scale drafts, therefore, in this study all the drafts

309 broader than 50 m (dashed lines) are included. The drafts narrower than 50 m are excluded
310 because most of them are turbulences ~~and they can hardly be resolved in models.~~

311 Fig. 5a shows the occurrence distributions as a function of the mean vertical velocity versus the
312 diameter of the drafts with the vertical velocity continuously $\geq 0.2 \text{ m s}^{-1}$ in magnitude. From the
313 figure, it is noted that many drafts narrower than 500 m have quite strong vertical velocities. The
314 maximum mean vertical velocity of these narrow drafts can reach 8 m s^{-1} , and the minimum
315 mean vertical velocity in the downdrafts is -6 m s^{-1} . With such strong mean vertical velocity,
316 narrow drafts could contribute noticeably to the total air mass flux. Fig. 5b presents the
317 occurrence distributions as a function of the air mass flux versus the diameter of the drafts. The
318 air mass flux is calculated as $\bar{\rho}\bar{w}D$ (LeMone and Zipser, 1980), where $\bar{\rho}$ is the mean air density
319 at the measurement temperature, \bar{w} is the mean vertical velocity and D is the diameter of each
320 draft. Due to the limitation of aircraft measurements, the air mass flux is calculated using the
321 data from single line penetrations. This may ~~not fully capture~~ introduce additional uncertainties
322 in the real air mass flux estimations in for these clouds and is a weakness of this study using
323 aircraft data. -Fig. 5b shows that the air mass flux in many drafts narrower than 500 m is actually
324 larger than that in some of the broader drafts. The maximum value for these narrow updrafts
325 reaches $4000 \text{ kg m}^{-1} \text{ s}^{-1}$, and the minimum value for the downdrafts reaches $-3000 \text{ kg m}^{-1} \text{ s}^{-1}$. The
326 normalized accumulated flux (red curves) reveals that the drafts narrower than 500 m (dotted
327 horizontal lines) make very significant contributions to the total air mass flux. Calculations
328 indicate that the updrafts narrower than 500 m contribute 20%–35% of the total upward flux, and
329 that the downdrafts narrower than 500 m contribute 50%–65% of the total downward air mass
330 flux. Drafts narrower than 50 m (dashed horizontal lines), which are excluded in this paper,
331 contributes less than 5% of the total air mass flux.

332 In this study, we delineate three different groups of updraft and downdraft using three thresholds
333 of air mass flux: $10 \text{ kg m}^{-1} \text{ s}^{-1}$, $100 \text{ kg m}^{-1} \text{ s}^{-1}$ and $500 \text{ kg m}^{-1} \text{ s}^{-1}$ in magnitude. The air mass flux
334 is used here to delineate the draft intensity because (1) air mass flux contains the information of
335 both vertical velocity and draft size; (2) air mass flux can reveal the vertical mass transport
336 through convections; and (3) air mass flux is an important component in cumulus and convection
337 parameterizations (e.g. Tiedtke, 1989; Bechtold et al., 2001). The first designated group, the
338 “weak draft,” with air mass flux $10\text{--}100 \text{ kg m}^{-1} \text{ s}^{-1}$ in magnitude, contributes 10% of the total
339 upward air mass flux and 10% of the total downward air mass flux. The “moderate draft,” with
340 air mass flux $100\text{--}500 \text{ kg m}^{-1} \text{ s}^{-1}$ in magnitude, contributes 25% of the total upward air mass flux
341 and 40% of the total downward air mass flux. The “strong draft,” where the air mass flux ≥ 500
342 $\text{kg m}^{-1} \text{ s}^{-1}$ in magnitude contributes 60% of the total upward air mass flux and 20% of the total
343 downward air mass flux. The definitions of “weak”, “moderate” and “strong” only apply for the
344 isolated convective clouds analyzed in this study, and are not necessarily appropriate for other
345 convections (e.g. MCS). Drafts weaker than $10 \text{ kg m}^{-1} \text{ s}^{-1}$ are not analyzed because they are too
346 weak and most of them are very narrow ~~and can hardly be resolved in models~~ (Fig. 5b). The
347 numbers of weak, moderate and strong updrafts and downdrafts sampled at 0–2 km, 2–4 km, 4–6
348 km, 6–8 km and 8–10 km MSL are shown in Table 2. Generally, weak and moderate drafts are
349 more often observed than strong drafts. At most of the height ranges, more updrafts are observed
350 than downdrafts.

351 Some researchers have defined a “draft core” by selecting the strongest portion in a draft. For
352 example, LeMone and Zipser (1980) define an updraft core as an ascending air motion with
353 vertical velocity continuously $\geq 1 \text{ m s}^{-1}$ and diameter $\geq 500 \text{ m}$. This definition of a “draft core” is
354 followed in a few more recent studies (e.g. Jorgensen and LeMone, 1989; Lucas et al., 1994;

355 Igau et al., 1999). We too analyzed the vertical air motion characteristics in the stronger portion
356 of the drafts considered here. However, we found that in many updrafts the strong portion where
357 the vertical velocity is continuously $\geq 1 \text{ m s}^{-1}$ dominates and contributes 80% of the total air
358 mass flux, so the statistics of the vertical air motion characteristics in the stronger portion are
359 very similar to those in the draft as a whole. Therefore, the present study focuses on “drafts” in
360 which both weak and strong portions are included.

361

362 **4. Results**

363 **4.1 Significance of drafts in different strengths**

364 From the analysis above, we note that relatively small and weak updrafts are frequently observed
365 in convective clouds. In this section, we provide further evidence to show the importance of the
366 relatively weak updrafts in terms of air mass flux.

367 Fig. 6a shows the average number of updrafts as a function air mass flux observed in the three
368 field campaigns. The solid, dashed and dotted lines represent the penetrations with different
369 diameters. As shown in Fig. 6a, weak and moderate updrafts are more often observed than strong
370 updrafts, and the numbers of updrafts are higher in longer penetrations. Since this is an average
371 result, the number of updrafts could be smaller than 1 (e.g. many narrow penetrations do not
372 have strong updrafts). Fig. 6b is similar to Fig. 6a but shows the occurrence frequency of
373 updrafts with different air mass fluxes (i.e. the vertical axis in Fig. 6a is normalized). For the
374 penetrations $< 1 \text{ km}$, many of the clouds only have weak or moderate updrafts, and [relatively](#)
375 strong updrafts are rarely observed. For penetrations of 1–10 km, the frequency of strong

376 updrafts increases and the frequency of weak and moderate updrafts decreases. For even longer
377 penetrations (>10 km), however, the frequency of weak updrafts increases again, indicating the
378 increasing importance of weak updrafts.

379 Fig. 7 shows the average percentile contributions to the total upward air mass flux by the three
380 different groups of updrafts as a function of penetration diameter. In Fig. 7a, all the penetrations
381 are included. Since many narrow clouds have no strong updrafts in terms of air mass flux, the
382 total air mass flux in these narrow clouds is mostly contributed by weak (red bar) and moderate
383 (green bar) drafts. These narrow clouds may have a high vertical velocity but small air mass flux.
384 As the diameter increases to 4 km, the contributions to total air mass flux from relatively weak
385 updrafts (red bar) decrease, while those from stronger updrafts (blue bar) increase. For a
386 penetration of 4 km, 80%–90% of the total upward mass flux is contributed by the strong
387 updrafts with air mass flux $\geq 500 \text{ kg m}^{-1} \text{ s}^{-1}$. However, for the penetrations with diameter larger
388 than 4 km, the contribution from relatively weak updrafts increases, probably because more
389 weak updrafts exist in wider clouds (Fig. 6). This is more obvious in Fig. 7b, in which only the
390 penetrations with at least one strong updraft are included. As the diameter increases from 400 m
391 to 20 km, the contribution from the weak and moderate updrafts (red bars and green bars)
392 increases from 2% to 20%. This suggests that as the cloud evolves and becomes broader (e.g.
393 mature or dissipating stage), the weak and moderate updrafts are also important and therefore
394 necessary to be considered in model simulations.

395

396 4.2 PDFs of vertical velocity and air mass flux

397 Fig. 8 shows the PDFs of the vertical velocity in the drafts sampled at 0–2 km, 2–4 km, 4–6 km
398 and higher than 6 km in the three field campaigns. Columns (a), (b) and (c) represent the drafts
399 with air mass flux $\geq 10 \text{ kg m}^{-1} \text{ s}^{-1}$, $\geq 100 \text{ kg m}^{-1} \text{ s}^{-1}$ and $\geq 500 \text{ kg m}^{-1} \text{ s}^{-1}$ in magnitude,
400 respectively; in other words, column (a) includes all the weak, moderate and strong of drafts,
401 column (b) includes moderate and strong updrafts, and column (c) includes strong updrafts only.
402 For statistical analysis, it is better to analyze different drafts together rather than separately.

403 Since the aircraft might not under sampled the strongest updraft cores, the tails of PDFs cannot
404 be plotted out to the tail could biased low, but these PDFs still provide some useful valuable
405 information. In all the panels, the vertical velocities are exponentially distributed for both
406 updrafts and downdrafts; the PDFs can be fitted using Eq. (1). From Fig. 8 we can see that at 0–2
407 km, the PDFs for both COPE and ICE-T are narrow; ~~the updrafts in COPE are slightly stronger~~
408 ~~than those in ICE-T, while the downdrafts are relatively weaker.~~ At 2–4 km, stronger updrafts
409 and broader PDFs are observed in both COPE and ICE-T compared to those at 0–2 km; the
410 maximum vertical velocity is about 15 m s^{-1} . In COPE, the downdrafts are stronger than those in
411 ICE-T, with the minimum vertical velocity as low as -10 m s^{-1} . For HiCu, the PDFs of the
412 vertical velocity at 2–4 km are narrow, because the HiCu was conducted in the High Plains and
413 the cloud bases are relatively high. At 4–6 km, the updrafts become stronger and the PDFs
414 become broader in all the three field campaigns compared to those at lower levels, especially for
415 COPE and ICE-T. Above 6 km, the PDFs for the updraft become broader in HiCu while they
416 slightly narrow in ICE-T compared to those at 4–6 km. For the downdrafts, the PDFs broaden
417 with height for all the three field campaigns. Generally, the PDFs of the vertical velocity are
418 similar for the three columns. The main difference is found in the first bins of the vertical
419 velocity ($0-2 \text{ m s}^{-1}$ and $-2-0 \text{ m s}^{-1}$): highest for column (a), which includes all the drafts with air

420 mass flux $\geq 10 \text{ kg m}^{-1} \text{ s}^{-1}$ in magnitude, lowest for column (c), which only includes the strong
421 drafts with air mass flux $\geq 500 \text{ kg m}^{-1} \text{ s}^{-1}$ in magnitude.

422 ~~Generally,~~ In Fig. 8, the updrafts are relatively stronger in ICE-T or COPE (maritime or coastal
423 convective clouds) than in HiCu (pure continental convective clouds). But notice the aircrafts
424 might not sample under sample the strongest part of the convective cores. In addition, the PDFs
425 are plotted as a function of MSL height ~~MSL,~~ the relatively narrow PDFs in HiCu compared to
426 COPE and ICE-T at the same height are possibly because of the higher cloud base in HiCu.
427 Other than the sample issues, the convention triggering mechanism is also important to the
428 updraft strength. The clouds sampled in the three field campaigns are all isolated convective
429 clouds, the CAPE in HiCu was smaller than in COPE and ICE-T. Previous studies (e.g. LeMone
430 and Zipser 1980; Heymsfield et al. 2010) suggest that for deeper convections (e.g. MCSs) the
431 updrafts were stronger in continental clouds than in maritime clouds., an observation that differs
432 from earlier studies (e.g. LeMone and Zipser 1980), in which stronger drafts were observed in
433 continental clouds. This is probably because in the previous field campaigns over ocean (e.g.
434 GATE), the aircraft did not penetrate the strongest cores due to safety concerns. Compared to
435 GATE project, in which the clouds were also sampled over tropical ocean, the PDFs of the
436 vertical velocity in ICE-T has a similar vertical dependence, broadening with height, ~~but~~ But
437 the PDFs are broader in ICE-T than those in GATE, and the maximum vertical velocity (25 m s^{-1})
438 in ICE-T is greater than that observed in GATE (15 m s^{-1}). Notice in GATE, the in-situ
439 measurements also have sampling issues. ~~In addition, convections in continental areas other than~~
440 ~~the High Plains (e.g. Great Plains) may be different from those in HiCu. Recently, Heymsfield et~~
441 ~~al. (2010) observed strong updrafts in both maritime and continental convective clouds: most~~
442 ~~exceed 15 m s^{-1} and some exceed 30 m s^{-1} , but the measurements were made for mature deep~~

443 ~~convection using airborne Doppler radar. More in-situ measurements are needed to further~~
444 ~~evaluate the difference between maritime and continental convective clouds, including both~~
445 ~~developing and mature stages.~~

446 ~~the convective available potential energy (CAPE) is larger in ICE-T than that in HiCu. Typically,~~
447 ~~the CAPE in ICE-T is greater than 2000 J kg⁻¹, and the CAPE in HiCu was less than 100 J kg⁻¹.~~
448 ~~However, CAPE in COPE is also low (typically less than 100 J kg⁻¹), which cannot explain the~~
449 ~~relatively strong vertical velocity. There are a few possible explanations for the stronger updrafts~~
450 ~~observed in ICE-T and COPE compared to those observed in HiCu. For example, the convective~~
451 ~~available potential energy (CAPE) is larger in ICE-T than that in HiCu. Typically, the CAPE in~~
452 ~~ICE-T is greater than 2000 J kg⁻¹, and the CAPE in HiCu was less than 100 J kg⁻¹. However,~~
453 ~~CAPE in COPE is also low (typically less than 100 J kg⁻¹), which cannot explain the relatively~~
454 ~~strong vertical velocity. The strong vertical velocity in ICE-T and COPE maybe also be related~~
455 ~~to ice initiation. There are many more millimeter drops in the convective clouds observed in~~
456 ~~ICE-T (Lawson et al., 2015) and COPE (Leon et al., 2015) than that in HiCu; the millimeter~~
457 ~~drops can result in fast ice initiation (Lawson et al., 2015), and the significant latent heat released~~
458 ~~during the ice initiation process can strengthen the vertical velocity. In addition, high~~
459 ~~concentrations of millimeter drops in ICE-T and COPE can result in the quick formation of~~
460 ~~graupel and frozen rain drops. The falling graupel and frozen rain drops can strongly enhance the~~
461 ~~ice generation through ice multiplication processes (Heymsfield and Willis, 2014) and possibly~~
462 ~~strengthen the updraft. Another difference among the three field campaigns is found in the~~
463 ~~downdrafts. The downdrafts in HiCu and COPE, which are sampled in mid-latitude convective~~
464 ~~clouds, are obviously stronger than those in ICE-T, which was conducted over tropical ocean.~~
465 ~~This may be because the ambient relative humidity is low in HiCu and COPE compared to ICE-~~

466 T, resulting in a faster evaporation of cloud drops and a stronger cooling effect when ambient air
467 mixes with cloud parcels through lateral entrainment (Heymsfield et al., 1978). But since the
468 diameters of the downdrafts in ICE-T are relatively broader (Fig. 4), the air mass fluxes of the
469 downdrafts are not obviously smaller than that in HiCu and COPE.

470 Fig. 9 shows the PDFs of the air mass flux for all the drafts sampled at 0–2 km, 2–4 km, 4–6 km
471 and higher than 6 km. The PDFs are exponentially distributed for the three field campaigns at
472 different heights, which can be fitted using Eq. (1). The coefficients for the fitted function are
473 shown in each panel. ~~At 0–2 km, the PDF of the air mass flux in the updrafts is relatively narrow
474 in ICE-T compared to that in COPE. For the downdraft, the PDF is broader in ICE-T than those
475 in COPE. As height increases up to 6 km, more updrafts with larger air mass flux are observed in
476 ICE-T and the PDFs broadens, but in COPE the PDFs remain similar. In HiCu, the PDFs for
477 updrafts broadens from 2–6 km then remain similar at altitudes higher than 6 km. For downdrafts,
478 the PDFs are similar at different heights for all the three field campaigns. Among the three field
479 campaigns, the differences of the PDFs are small for the weak and moderate drafts and are larger
480 for the strong drafts.~~In the three field campaigns, the PDFs of air mass flux have no obvious
481 trend with height, although the PDFs of diameter and vertical velocity are broadening with
482 height. The differences among the three field campaigns are small for weak and moderate drafts,
483 and become slightly larger for relatively strong updrafts, but again notice there are which could
484 be resulted from the sampling issues.

485

486 4.3 Profiles of vertical velocity and air mass flux

487 Fig. 10 is a Whisker-Box plot showing the profiles of the vertical velocity (a-c) and air mass flux
488 (d-f) in the drafts based on the three defined thresholds of air mass flux. The solid box includes
489 all the three different groups of drafts, the dashed boxes excludes the weak drafts, and the dotted
490 boxes includes strong drafts only. The minimum, 10%, 50%, 90% and the maximum values are
491 shown in each box. ~~Notice that the vertical velocity and air mass flux in the downdraft is~~
492 ~~negative, so the minimum value represents the strongest subsiding parcel, the 10% value~~
493 ~~represents the strongest 10th percentile subsiding parcel, and the 90% value represents the~~
494 ~~weakest 10th percentile subsiding parcel. This is opposite to the updraft.~~ In each panel, the
495 absolute values of the vertical velocities and air mass flux (except the minimum and maximum
496 ones) are relatively small for the solid boxes.

497 In Fig. 10a-c, the three definitions of drafts show different intensities in the vertical velocities.
498 Typically, the 10%, 50% and 90% values in the dotted boxes are 1–2 times larger in magnitude
499 than those in the solid boxes. However, the profiles of the three definitions of drafts vary
500 similarly with height for each field campaign. In the updrafts sampled during HiCu (Fig. 10a),
501 the maximum vertical velocity increases ~~from about 10 m s⁻¹ to 18 m s⁻¹~~ with height up to 8 km,
502 then decreases [with height](#); the 90% vertical velocity in the solid boxes increases from 4 m s⁻¹ to
503 8 m s⁻¹ between 0–10 km. The 10% and 50% vertical velocities in the solid boxes remain similar
504 between 2–8 km then slightly increase at 8–10 km. ~~The magnitudes of the 10% and 50% vertical~~
505 ~~velocities in the solid boxes are about 0.5–0.6 m s⁻¹ and 1.8–2.5 m s⁻¹.~~ In the downdrafts, the
506 minimum vertical velocity decreases from –7 m s⁻¹ to –12 m s⁻¹ up to 8 km and increases to –9 m
507 s⁻¹ at 8–10 km. The 10%, 50 % and 90% values all slightly decrease with height. In the updrafts
508 sampled during COPE (Fig. 10b), the maximum ~~vertical velocities increase from 8 m s⁻¹ to 23 m~~
509 ~~s⁻¹ between 0–6 km, the~~ 10%, 50% and 90% vertical velocities increase ~~up to 6 km~~ [with height](#),

510 the maximum value is 23 m s⁻¹ ~~The magnitudes are 0.35–0.45 m s⁻¹, 1–1.6 m s⁻¹, and 2.6–6 m s⁻¹~~
511 ~~in the solid boxes, respectively.~~ The minimum vertical velocity in the downdrafts intensifies
512 from –5 to –10 m s⁻¹ with height up to 4 km, then remains similar at 4–6 km. In the updrafts
513 sampled during ICE-T (Fig. 10c), the maximum vertical velocities increase with height from 5.5
514 m s⁻¹ to 25 m s⁻¹ up to 6 km, then slightly decreases at 6–8 km. The 90% value increases from 2
515 to 6 m s⁻¹ between 0–4 km, then remains similar at higher levels. The 10% and 50% values;
516 ~~which are about 0.32–0.6 m s⁻¹ and 0.8–1.8 m s⁻¹ in the solid boxes, respectively,~~ do not show an
517 obvious trend with height. In the downdrafts the minimum vertical velocity remains similar
518 below ~~increases from –6 m s⁻¹ to –5 m s⁻¹ between 0 km and 4 km,~~ and decreases ~~from –5 m s⁻¹~~
519 to –18 m s⁻¹ between 4 km and 8 km. The 10%, 50% and 90% values tend to decrease or remain
520 similar at first and then increase with height. The peak (~25 m s⁻¹) and the minimum (~–18 m s⁻¹)
521 vertical velocities are observed at 4–6 km and 6–8 km, respectively.

522 To summarize, vertical velocity in the drafts varies differently with height in the three field
523 campaigns. ~~Generally, the maximum and 90% vertical velocities in the updrafts are greater in~~
524 ~~COPE or ICE-T than in HiCu, while the median vertical velocities are the greatest in HiCu and~~
525 ~~weakest in ICE-T.~~ Stronger downdrafts are often observed in HiCu and COPE compared to those
526 in ICE-T. The weak, moderate and strong drafts have similar variations ~~of the vertical velocity~~
527 with height, but the magnitudes are the smallest when including all the drafts and become larger
528 if the weak drafts are excluded. The 10%, 50% and 90% vertical velocities in updrafts and
529 downdrafts over tropical ocean (ICE-T) observed in this study generally have similar magnitudes
530 to those shown in previous studies (e.g. LeMone and Zipser, 1980; Lucas and Zipser, 1994). But
531 strong updrafts (downdrafts) in excess of 20 m s⁻¹ (–10 m s⁻¹) are also observed in this study,
532 which are ~~not rarely shown reported~~ not rarely shown reported in previous aircraft observations. This finding is consistent

533 with recent remote sensing observations (e.g. Heymsfield et al., 2009). The updrafts and
534 downdrafts in convective clouds over land shown in this study (HiCu) are weaker than those
535 shown by Byers and Braham (1949) and Heymsfield et al. (2009), possibly because the clouds
536 sampled in HiCu were isolated convective clouds over high plains, which could be different than
537 deeper convective clouds from low elevations.~~of the sampling issues, different convection~~
538 ~~mechanisms and the relatively small CAPE in HiCu. HiCu was conducted over the High Plains.~~

539 Fig. 10d-f shows the profiles the air mass flux statistics for the drafts sampled during the three
540 field campaigns. As expected, the absolute values of the air mass flux are relatively small if all
541 the drafts are included (dotted boxes), and become larger if the drafts with small air mass flux are
542 excluded. However, the variations of the air mass flux with height are similar for the three
543 different definitions in each panel. As determined by the three thresholds, the minimum absolute
544 values in the solid boxes are about 10 times smaller than those in the dashed boxes and about 50
545 times smaller than those in the dotted boxed; for the 10%, 50%, 90% and the maximum absolute
546 values, the differences among the three type of boxes become smaller. ‡The air mass flux varies
547 with height differently for the three field campaigns and do not have obvious trend with height.
548 For updraft, the maximum air mass flux is of the order of $10^4 \text{ kg m}^{-1} \text{ s}^{-1}$, and the median values
549 for the three different types of boxes are typically $\sim 100 \text{ kg m}^{-1} \text{ s}^{-1}$, $\sim 200 \text{ kg m}^{-1} \text{ s}^{-1}$ and $\sim 1000 \text{ kg}$
550 $\text{m}^{-1} \text{ s}^{-1}$, respectively. The air mass flux in the downdrafts is a few times smaller in magnitude
551 than those in the updrafts, but extreme strong downdraft on the order of $10^4 \text{ kg m}^{-1} \text{ s}^{-1}$ may could
552 be observed in some specific cases. Compared to previous studies, the air mass flux in this study
553 shows similar magnitudes, but the vertical dependences are different. Lucas and Zipser (1994)
554 show that the convection off tropical Australia intensifies with height from 0 to 3 km, then
555 weakens with height in terms of air mass flux. Anderson et al. (2005) shows that updrafts and

556 downrafts over the tropical Pacific Ocean intensify with height up to 4 km, then weaken at
557 higher levels. In contrast, this study shows the strongest updrafts and downrafts in terms of air
558 mass flux were observed at higher levels.~~In the present study, the strongest updrafts and~~
559 downrafts are observed at higher levels for all the three field campaigns.

560 ~~In HiCu, the air mass flux does not show an obvious trend with height. In the updraft, the 10%,~~
561 ~~50% and 90% values remain similar at different height ranges. The maximum air mass flux~~
562 ~~increases from 2–6 km, then decreases with height. The peak value is about $1.3 \times 10^4 \text{ kg m}^{-1} \text{ s}^{-1}$,~~
563 ~~found at 4–6 km. The air mass flux in the downrafts has relatively larger variability, especially~~
564 ~~for the minimum values. The strongest downraft in terms of air mass flux (about $1.2 \times 10^4 \text{ kg}$~~
565 ~~$\text{m}^{-1} \text{ s}^{-1}$) is found at 4–6 km, but this is probably due to a specific case since the 50% and 90%~~
566 ~~values are similar to those at the other height ranges. In COPE, the 90% and the maximum air~~
567 ~~mass flux in the updraft tend to increase with height, while the 10% and 50% values are similar~~
568 ~~at different height ranges. For the downraft, the minimum air mass flux decreases between 0–2~~
569 ~~km and remains similar at 4–6 km. The 10%, 50% and 90% values are similar at different height~~
570 ~~ranges. The strongest updrafts and downrafts in terms of air mass flux are observed at 4–6 km~~
571 ~~and 2–4 km, about $1.8 \times 10^4 \text{ kg m}^{-1} \text{ s}^{-1}$ and $2.8 \times 10^3 \text{ kg m}^{-1} \text{ s}^{-1}$. In ICE-T, the maximum air mass~~
572 ~~flux in the updraft increases with height up to 6 km, then decreases at 6–8 km. The 10%, 50%~~
573 ~~and 90% values in the updraft and downraft intensify from 0–4 km and decrease or remain~~
574 ~~similar at higher levels. The strongest updraft ($3 \times 10^4 \text{ kg m}^{-1} \text{ s}^{-1}$) and downraft ($3.5 \times 10^3 \text{ kg m}^{-1}$~~
575 ~~s^{-1}) are observed at 4–6 km and 0–2 km, respectively. The minimum value is probably due to a~~
576 ~~specific case because the 10%, 50% and 90% values at 0–2 km are larger or similar to those at~~
577 ~~the other heights.~~

578 ~~To summarize, the air mass flux varies with height differently for the three field campaigns. For~~
579 ~~updraft, the maximum air mass flux is of the order of $10^4 \text{ kg m}^{-1} \text{ s}^{-1}$, and the median values for~~
580 ~~the three different types of boxes are typically $100 \text{ kg m}^{-1} \text{ s}^{-1}$, $200 \text{ kg m}^{-1} \text{ s}^{-1}$ and 1000 kg m^{-1}~~
581 ~~ s^{-1} , respectively. The air mass flux in the downdrafts is a few times smaller in magnitude than~~
582 ~~those in the updrafts, but extreme strong downdraft on the order of $10^4 \text{ kg m}^{-1} \text{ s}^{-1}$ may be~~
583 ~~observed in some specific cases. Compared to previous studies, the air mass flux in this study~~
584 ~~shows similar magnitudes, but the vertical dependences are different. Lucas and Zipser (1994)~~
585 ~~show that the convection off tropical Australia intensifies with height from 0 to 3 km, then~~
586 ~~weakens with height in terms of air mass flux. Anderson et al. (2005) shows that updrafts and~~
587 ~~downdrafts over the tropical Pacific Ocean intensify with height up to 4 km, then weaken at~~
588 ~~higher levels in terms of air mass flux. In the present study, the strongest updrafts and~~
589 ~~downdrafts are observed at higher levels for all the three field campaigns.~~

590

591 **4.4 Composite structure of vertical velocity**

592 Fig. 11- shows the composite structure for the updrafts and downdrafts with air mass flux > 10
593 $\text{ kg m}^{-1} \text{ s}^{-1}$ as a function of normalized scale. The 0 and 1 coordinates on the x-axis indicate the
594 upwind and downwind sides of the draft. Since we do not have continuous penetrations in a
595 single cloud, we have to statistically analyze the evolution of the draft structure. In Fig. 11, we
596 can see the normalized shape do not have significant change with height, the peak vertical
597 velocity is strengthening with height for all the three field campaigns. If the magnitude of the
598 vertical velocity is normalized, the structures of the updraft and downdraft at different heights
599 will be very similar. Connecting this figure to the PDFs of diameter (Fig. 4) and air mass flux

600 (Fig. 9), the results show statistically that the drafts were expanding (Fig. 4) and the vertical
601 velocity was strengthening (Fig. 11), but the air mass flux was not increasing with height (Fig. 9).
602 This reveals the complexity of the evolution of the drafts. Based on our datasets, there could be
603 different possibilities of the updraft evolution: 1) an updraft expands and the vertical velocity
604 weakens with height, 2) an updraft expands and the vertical velocity strengthens with height, 3)
605 an updraft splits to multiple updrafts and downdrafts, 4) two updrafts merged and become one
606 updrafts. In addition, entrainment/detrainment and water loading also have important impacts on
607 ~~the evolution of drafts in convective clouds. shows the composite structure of the vertical velocity~~
608 ~~as a function of the normalized diameter for the updrafts and downdrafts with air mass flux ≥ 10~~
609 ~~$\text{kg m}^{-1}\text{s}^{-1}$, $100 \text{ kg m}^{-1}\text{s}^{-1}$ and $500 \text{ kg m}^{-1}\text{s}^{-1}$ in magnitude. As expected, the draft as a whole is~~
610 ~~weaker if all the drafts are included in the calculation and becomes stronger if the drafts with~~
611 ~~small air mass flux are excluded. In HiCu, when all weak, moderate and strong updrafts are~~
612 ~~included (red curves), the vertical velocity near the center is about 1.7 m s^{-1} . When only~~
613 ~~moderate and strong updrafts are included (green curves), the vertical velocity near the center is~~
614 ~~$\sim 2.4 \text{ m s}^{-1}$. When all the updrafts with air mass flux smaller than $500 \text{ kg m}^{-1}\text{s}^{-1}$ in magnitude are~~
615 ~~excluded, the absolute values of the vertical velocity near the center increase to $\sim 3.4 \text{ m s}^{-1}$. The~~
616 ~~vertical velocity in downdrafts is about 0.2 m s^{-1} smaller in magnitude than that in updrafts. The~~
617 ~~structures of the vertical velocity in COPE are quite similar to those in HiCu, in both shape and~~
618 ~~magnitude, especially for the red and green curves. The blue curves have relatively larger~~
619 ~~variations due to the small sample size. These variations reveal the complicated structure in some~~
620 ~~drafts. In ICE T, the shapes of the vertical velocity structures are similar to those in HiCu and~~
621 ~~COPE, but the magnitudes are smaller, which suggests that statistically more weak drafts are~~
622 ~~found in ICE T, although the peak vertical velocity is observed in ICE T. This is consistent with~~

623 ~~Fig. 10. In Fig. 11, if the magnitude of the vertical velocity is normalized, the structures of the~~
624 ~~three defined classes of updraft and downdraft among the three field campaigns will be very~~
625 ~~similar.~~

626 In this composite analysis based on in-situ measurements, the penetration direction has no
627 obvious impact on the vertical velocity structure, whether the aircraft penetrates along or across
628 the horizontal wind ([not shown](#)). For convective cloud, wind shear has a large impact on the
629 cloud evolution (Weisman and Klemp 1982); however, aircraft data are insufficient to reveal the
630 wind shear impact, because each penetration is made at a single level and the aircraft does not
631 always penetrate through the center of the draft. Remote sensing data can be helpful to study the
632 two-dimensional or three-dimensional structures of the vertical velocity in convective clouds.
633 [For example, airborne radar with slant and zenith/nadir viewing beams can provide two-](#)
634 [dimensional wind structure in convective clouds](#) (e.g. Wang and Geerts, 2013). [Volumetric radar](#)
635 [\(e.g. Collis et al. 2013, Jorgensen et al. 2000\) can provide three-dimensional structure of air \(or](#)
636 [hydrometeor\) motion](#). Thus, in-situ measurements as well as remote sensing measurements are
637 needed to further analyze the wind shear impact.

638

639 **4.5 Vertical air motion characteristics as clouds evolve**

640 Fig. 12 shows the profiles of the vertical velocity (a-c) and the air mass flux (d-f) for the updraft
641 and downdraft in the convective clouds with different cloud top heights (CTH). Here, all weak,
642 moderate and strong updrafts are included. Different colors represent the clouds with different
643 CTHs. These profiles can generally reveal the change of vertical velocity and air mass flux as the
644 clouds evolve. The key point presented in Fig. 12[a-c](#) is that the peak vertical velocity ~~and air~~

645 ~~mass flux~~ is observed at higher levels as the clouds evolve. For clouds with CTHs lower than 4
646 km (red boxes), the maximum vertical velocity is observed at 2–4 km. When the cloud become
647 deeper, the vertical velocity and air mass flux are stronger at higher levels. This is to be expected,
648 because all the data analyzed in this paper are collected from isolated convective clouds, so the
649 convective bubbles keep ascending as the clouds evolve. MCSs may have different
650 characteristics of vertical air motion because there is continuous low level convective source.
651 The maximum vertical velocity is observed within 2 km below cloud top; this is consistent with
652 Doppler velocity images measured by WCR (e.g. Fig. 2b), which show the typical strongest
653 updraft is observed 1–1.5 km below cloud top. The strongest downdrafts are sometimes observed
654 more than 2 km below cloud top. The 10% and 50% values do not have obvious trend as the
655 clouds evolve, ~~especially in HiCu and ICE-T~~, possibly because of the increasing contribution
656 from moderate and weak drafts as the clouds become deeper and broader (Fig. 6 and 7). The air
657 mass flux (Fig. 12d-f) has no obvious trend as the clouds evolve, again suggesting multiple
658 factors (e.g. entrainment/detainment, microphysics) have impact on the evolution of the drafts.
659 ~~Generally, in HiCu and ICE-T the drafts intensify as the clouds evolve, but this is not found in~~
660 ~~COPE, maybe because most of the penetrations were made near the cloud top, rather than in the~~
661 ~~strongest portion of a draft. Since the aircraft just provides a line of data through drafts, and not~~
662 ~~vertical information unless the plane makes multiple passes through the same cell, more data,~~
663 ~~including remote sensing measurements are needed to better understand the evolution of the~~
664 ~~vertical velocity in convective clouds at different stages. ~~Since the vertical resolution of aircraft~~~~
665 ~~~~in situ data is poor, more data, including remote sensing measurements, are needed to better~~~~
666 ~~~~understand the evolution of the vertical velocity in convective clouds as they go through the~~~~
667 ~~~~different stages..~~~~

668

669 **5. Discussion**

670 In this study, we provide the statistics of vertical air motion in isolated convective clouds using
671 in-situ measurements from three field campaigns. The statistical results suggest vertical air
672 motions in convective clouds are very complicated and could be affected by many factors.

673 Microphysics strongly interacts with vertical velocity through different processes, for example,
674 droplet condensation/evaporation, ice nucleation/sublimation, water loading, etc. Yang et al.
675 (2016) shows the LWC and IWC are both higher in stronger updrafts in developing convective
676 clouds, while the liquid fraction has no obvious correlation with vertical velocity. In mature
677 convective clouds the LWC is also higher in stronger updrafts, but the IWC is similar in
678 relatively weak and strong updrafts, the liquid fraction is correlated to the vertical velocity
679 between -3 C and -8 C, possibly because Hallet-Mossop process is more significant in weaker
680 updrafts (Heymsfield and Willis, 2014). Lawson et al. (2015) shows the existence of millimeter
681 drops in the convective clouds ~~drops~~ can result in fast ice initiation, and the significant latent
682 heat released during the ice initiation process can strengthen the updrafts. In ~~in~~ ICE-T and COPE,
683 we do observe many millimeter drops, which may strongly interact with vertical velocity through
684 fast ice generation. However, in some cases, the existence of millimeter drops can result in
685 strong warm rain process (Yang et al. 2016; Leon et al. 2016), which may weaken the updrafts
686 and make the clouds dissipate quickly.

687 Entrainment/detrainment also has strong interaction with the vertical velocity. In the analysis
688 above, we see the downdrafts in HiCu and COPE are obviously stronger than those in ICE-T.
689 This maybe partly because the ambient relative humidity is low in HiCu and COPE compared to

690 ICE-T, resulting in a strong evaporation-cooling effect when ambient air mixes with cloud
691 parcels through lateral entrainment/detrainment (Heymsfield et al., 1978). Entrainment has
692 impact on updrafts as well. Recent study using in-situ measurement and model simulation
693 suggests stronger entrainment may result in weaker updrafts (Lu et al., 2016). In ICE-T, we also
694 find the weaker updrafts are associated with stronger entrainment/detrainment using in-situ
695 measurements of relative humidity, equivalent potential temperature, droplet concentration and
696 LWC (not shown). In COPE and HiCu, we do not have the appropriate instruments to do similar
697 analyses. Previous studies (e.g. Heymsfield et al., 1978; Wang et al., 2013) suggest updraft cores
698 unaffected by entrainment may exist in some convective clouds.

699 ~~A~~ ~~Here we again~~ it is important to be aware of ~~highlight there are many~~ limitations ~~and sampling~~
700 ~~issues~~ of using aircraft in-situ measurements for this kind of study. More observations (in situ
701 and remote sensing) as well as model simulations are needed to better characterize the vertical
702 air motion in convective clouds and its interactions with microphysics and
703 entrainment/detrainment mixing.

704

705 **5.6. Conclusions**

706 The vertical velocity and air mass flux in isolated convective clouds are statistically analyzed in
707 this study using aircraft data collected from three field campaigns, HiCu, COPE and ICE-T,
708 conducted over mid-latitude High Plains, mid-latitude coastal area and tropical ocean. Three
709 thresholds of air mass flux are selected to delineate weak, moderate and strong draft: $10 \text{ kg m}^{-1} \text{ s}^{-1}$,
710 $100 \text{ kg m}^{-1} \text{ s}^{-1}$ and $500 \text{ kg m}^{-1} \text{ s}^{-1}$ in magnitude. These definitions only apply for the isolated

711 [convective cloud in this study and are not necessarily appropriate for other convections \(e.g.](#)
712 [MCSs\)](#). The main findings are as follows.

713 1) Small-scale updrafts and downdrafts in convective clouds are often observed in the three
714 field campaigns. More than 85%, 90% and 74% of the updrafts are narrower than 500 m in HiCu,
715 COPE and ICE-T, respectively, and more than 90 % of the downdrafts are narrower than 500 m
716 in the three field campaigns combined. These small scale drafts make significant contributions to
717 the total air mass flux. Updrafts narrower than 500 m contribute 20%–35% of the total upward
718 flux, and downdrafts narrower than 500 m contribute 50%–65% of the total downward air mass
719 flux.

720 2) In terms of the air mass flux, the weak and moderate drafts make an important
721 contribution to the total air mas flux exchange. Generally, the number of drafts increases with
722 cloud diameter. For many narrow clouds, the weak and moderate drafts dominate and contribute
723 most of the total air mass flux. For broader clouds, the stronger updrafts contribute most of the
724 total air mass flux, but the contribution from weak and moderate drafts increases as the cloud
725 evolves.

726 3) PDFs and profiles of the vertical velocity are provided for the ~~three defined types of~~
727 drafts. In all the height ranges, the PDFs are roughly exponentially distributed. ~~At the lowest~~
728 ~~level, the PDFs of the vertical velocity~~ [and](#) ~~are relatively narrow, and~~ broaden with height. ~~For~~
729 ~~the updrafts, the PDFs of the vertical velocity are broader in ICE-T and COPE, while for the~~
730 ~~downdrafts the PDFs of the vertical velocity are broader in HiCu and COPE. The profiles show~~
731 ~~that updrafts are stronger in ICE-T and COPE than in HiCu, and d~~ [The](#) downdrafts are stronger in
732 HiCu and COPE compared to ICE-T. [Relatively strong updrafts \(\$> 20 \text{ m s}^{-1}\$ \) were sampled](#)

733 during ICE-T and COPE. The updrafts in HiCu are weaker than previous studies of deeper
734 continental convections, possibly because the clouds sampled in HiCu were isolated convective
735 clouds over high plains, which could be different than deeper convective clouds from low
736 elevations.

737 4) PDFs and profiles of the air mass flux are provided for the drafts. The PDFs are similarly
738 exponentially distributed at different heights, and have no obvious trend with height. ~~For~~
739 ~~updrafts, the PDFs are broader in ICE-T than in HiCu and COPE, but for downdrafts the PDFs~~
740 ~~are broader in HiCu and COPE than in ICE-T.~~ In the updrafts, the maximum air mass flux has an
741 order of $10^4 \text{ kg m}^{-1} \text{ s}^{-1}$. The air mass flux in the downdrafts are typically a few times smaller in
742 magnitude than those in the updrafts.

743 5) The composite structures of the vertical velocity in the updrafts and downdrafts have
744 similar normalized shapes for the three field campaigns: the vertical velocity is the strongest near
745 the center, and weakens towards the edges. ~~On average, the updrafts have similar intensity across~~
746 ~~the three field campaigns, while for downdrafts the vertical velocity is the weakest in ICE-T and~~
747 ~~stronger in HiCu and COPE~~ Statistically, the vertical velocity and diameter were increasing with
748 height, but the air mass flux does not has obvious trend with height, suggesting
749 ~~entrainment~~ suggesting entrainment/detrainment, water loading and other complicated processes
750 have impacts on the evolution of the drafts.-

751 6) The change of vertical air motion characteristics as the cloud evolves are briefly
752 discussed. Generally, the strongest portion of a draft ascends with height as the cloud evolves.
753 The maximum vertical velocity is observed within 2 km below cloud top; the downdrafts are
754 sometimes stronger at levels more than 2 km below cloud top.

755 The vertical air motion in convective clouds is very complicated, and is affected by many factors,
756 such as convection mechanisms, entrainment/detrainment and microphysics. ~~Based on the~~
757 ~~aircraft observations from three field campaigns, this study provides quantitative analyses of the~~
758 ~~vertical air motion characteristics in isolated convective clouds, compares the differences of~~
759 ~~vertical velocity and air mass flux among the different field campaigns, and shows the~~
760 ~~importance of small-scale updrafts and downdrafts. The results are useful to evaluate model~~
761 ~~simulations and improve parameterizations in models.~~ This study only deals with a biased
762 sample of isolated convective clouds and there are many several limitations associated with using
763 of aircraft in-situ measurements. More data, including in-situ and remote sensing measurements,
764 are needed ~~To to~~ better understand the ~~differences of the vertical air motions among different~~
765 ~~convective clouds and the evolution of the updrafts and downdrafts in~~ vertical air motion in
766 convective clouds ~~more data are needed.~~

767

768 **Acknowledgments**

769 This work is supported by National Science Foundation Award: AGS-1230203 and AGS-
770 1034858, the National Basic Research Program of China under grant no. 2013CB955802 and
771 DOE Grant DE-SC0006974 as part of the ASR program. The authors acknowledge the crew of
772 NCAR C-130 and University of Wyoming King Air for collecting the data and for providing
773 high-quality products. Many thanks are also extended to the two reviewers for their constructive
774 comments.

775

776 **References**

- 777 Anderson, N. F., Grainger, C. A., and Stith, J. L.: Characteristics of Strong Updrafts in
778 Precipitation Systems over the Central Tropical Pacific Ocean and in the Amazon. *J. Appl.*
779 *Meteor.*, 44, 731–738, 2005.
- 780 Arakawa, A.: The cumulus parameterization problem: Past, present, and future. *J. Clim.*, 17,
781 2493–2525, 2004.
- 782 Bechtold, P., Bazile, E., Guichard, F., Mascart, P. and Richard, E.: A mass-flux convection
783 scheme for regional and global models. *Quarterly Journal of the Royal Meteorological*
784 *Society*, 127(573), 869-886, 2001.
- 785 Byers, H. R. and Braham, R. R.: The Thunderstorm-Report of the Thunderstorm Project. U.S.
786 Weather Bureau, Washington, D.C., Jun 1949. 287 pp. [NTIS PB234515], 1949.
- 787 Del Genio, A. D., Wolf, A. B., and Yao, M.-S.: Evaluation of regional cloud feedbacks using
788 single-column models, *J. Geophys. Res.*, 110, D15S13, doi:10.1029/2004JD005011, 2005.
- 789 [Collis, S., Protat, A., May, P. T., and Williams, C.: Statistics of Storm Updraft Velocities from](#)
790 [TWP-ICE Including Verification with Profiling Measurements. *J. Appl. Meteor. Climatol.*, 52,](#)
791 [1909–1922, 2013.](#)
- 792 Donner, L. J., Seman, C. J., Hemler, R. S., and Fan, S.: A Cumulus Parameterization Including
793 Mass Fluxes, Convective Vertical Velocities, and Mesoscale Effects: Thermodynamic and
794 Hydrological Aspects in a General Circulation Model. *J. Climate*, 14, 3444–3463, 2001.

795 [Giangrande, S. E., Collis, S., Straka, J., Protat, A., Williams, C. and Krueger, S.: A summary of](#)
796 [convective-core vertical velocity properties using ARM UHF wind profilers in Oklahoma. *J. App.*](#)
797 [Meteor. Climatol.](#), 52, 2278-2295, 2013.

798 Heymsfield, A. J., Johnson, P. N., and Dye, J. E.: Observations of Moist Adiabatic Ascent in
799 Northeast Colorado Cumulus Congestus Clouds. *J. Atmos. Sci.*, 35, 1689–1703, 1978.

800 Heymsfield, A. J., and Willis, P.: Cloud conditions favoring secondary ice particle production in
801 tropical maritime convection. *J. Atmos. Sci.*, 71, 4500–4526, 2014.

802 Heymsfield, G. M., Tian, L., Heymsfield, A. J., Li, L., and Guimond, S.: Characteristics of Deep
803 Tropical and Subtropical Convection from Nadir-Viewing High-Altitude Airborne Doppler
804 Radar. *J. Atmos. Sci.*, 67, 285–308, 2010.

805 Hildebrand, P. H., Lee, W., Walther, C. A., Frush, C., Randall, M., Loew, E., Neitzel, R., and
806 Parsons, R.: The ELDORA/ASTRAIA Airborne Doppler Weather Radar: High-Resolution
807 Observations from TOGA COARE. *Bull. Amer. Meteor. Soc.*, 77, 213–232, 1996

808 Hogan, R. J., Grant, A. L., Illingworth, A. J., Pearson, G. N., and O’Connor, E. J.: Vertical
809 velocity variance and skewness in clear and cloud-topped boundary layers as revealed by
810 Doppler lidar, *Q. J. Roy. Meteorol. Soc.*, 135, 635–643, 2009.

811 Houze Jr., R. A., and Betts, A. K.: Convection in GATE, *Rev. Geophys.*, 19(4), 541–576, 1981.

812 Igau, R. C., LeMone, M. A., and Wei, D.: Updraft and Downdraft Cores in TOGA COARE:
813 Why So Many Buoyant Downdraft Cores?. *J. Atmos. Sci.*, 56, 2232–2245, 1999.

814 Ivanova, I. T. and Leighton, H. G.: Aerosol–Cloud Interactions in a Mesoscale Model. Part I:
815 Sensitivity to Activation and Collision–Coalescence. *J. Atmos. Sci.*, 65, 289–308, 2008.

816 Jorgensen, D. P., Zipser, E. J., and LeMone, M. A.: Vertical Motions in Intense Hurricanes. *J.*
817 *Atmos. Sci.*, 42, 839–856, 1985.

818 Jorgensen, D. P. and LeMone, M. A.: Vertically Velocity Characteristics of Oceanic Convection.
819 *J. Atmos. Sci.*, 46, 621–640, 1989.

820 [Jorgensen, D. P., and Smull, B. F.: Mesovortex circulations seen by airborne Doppler radar](#)
821 [within a bow-echo mesoscale convective system. *Bull. Amer. Meteor. Soc.*, 74, 2146–2157,](#)
822 [1993.](#)

823 [Jorgensen, D. P., Shepherd, T. R., and Goldstein, A. S.: A dual-pulse repetition frequency](#)
824 [scheme for mitigating velocity ambiguities of the NOAA P-3 airborne Doppler radar. *J. Atmos.*](#)
825 [Oceanic Technol., 17, 585–594, 2000.](#)

826 Khairoutdinov, M. F., Krueger, S. K., Moeng, C.-H., Bogenschutz, P. A., and Randall, D. A.:
827 Large-Eddy Simulation of Maritime Deep Tropical Convection, *J. Adv. Model. Earth Syst.*, 1, 15,
828 doi:10.3894/JAMES.2009.1.15, 2009.

829 Khelif, D., Burns, S. P., and Friehe, C. A.: Improved Wind Measurements on Research
830 Aircraft. *J. Atmos. Oceanic Technol.*, 16, 860–875, 1999.

831 Kollias, P and Albrecht, B.: Vertical Velocity Statistics in Fair-Weather Cumuli at the ARM
832 TWP Nauru Climate Research Facility. *J. Climate*, 23, 6590–6604, 2010.

833 Lawson, P. R., Woods, S., and Morrison, H.: The microphysics of ice and precipitation
834 development in tropical cumulus clouds. *J. Atmos. Sci.*, 72, 2429-2445, 2015.

835 LeMone, M. A., and Zipser, E. J.: Cumulonimbus vertical velocity events in GATE. Part I:
836 Diameter, intensity and mass flux. *J. Atmos. Sci.*, 37, 2444–2457, 1980.

837 Leon, D., and co-authors: The CONvective Precipitation Experiment (COPE): Investigating the
838 origins of heavy precipitation in the southwestern UK. *Bull. Amer. Meteor. Soc.*
839 doi:10.1175/BAMS-D-14-00157.1, in press, 2016.

840 [Lu, C., Liu, Y., Zhang, G. J., Wu, X., Endo, S., Cao, L., Li, Y. and Guo, X.: Improving](#)
841 [parameterization of entrainment rate for shallow convection with aircraft measurements and](#)
842 [large eddy simulation. *J. Atmos. Sci.*, 2015.](#)

843 Lucas, C., Zipser, E. J., and Lemone, M. A.: Vertical Velocity in Oceanic Convection off
844 Tropical Australia. *J. Atmos. Sci.*, 51, 3183–3193, 1994.

845 May, P. T. and Rajopadhyaya, D. K.: Vertical Velocity Characteristics of Deep Convection over
846 Darwin, Australia. *Mon. Wea. Rev.*, 127, 1056–1071, 1999.

847 [Nicol, J. C., Hogan, R. J., Stein, T. H. M., Hanley, K. E., Clark, P. A., Halliwell, C. E., Lean, H.](#)
848 [W., and Plant, R. S.: Convective updraught evaluation in high-resolution NWP simulations using](#)
849 [single-Doppler radar measurements. *Q. J. R. Meteorol. Soc.*, 141, 3177–3189, 2015.](#)

850 Schmeter, S. M.: Structure of fields of meteorological elements in a cumulonimbus zone, *Hydro.*
851 *Meteor. Serv., Trans. Cent. Aerol. Obs.* [Trans. From Russian by Israel Prog. For Sci. Trans.,
852 Jerusalem, 1970, 117 pp.], 1969.

853 Schumacher, C., Stevenson, S. N., and Williams, C. R.: Vertical motions of the tropical
854 convective cloud spectrum over Darwin, Australia. *Q.J.R. Meteorol. Soc.*. doi: 10.1002/qj.2520,
855 2015.

856 Tiedtke, M.: A comprehensive mass flux scheme for cumulus parameterization in large-scale
857 models. *Monthly Weather Review*, 117(8), 1779-1800, 1989.

858 Tonttila, J., O'Connor, E. J., Niemelä, S., Räisänen, P., and Järvinen, H.: Cloud base vertical
859 velocity statistics: a comparison between an atmospheric mesoscale model and remote sensing
860 observations. *Atmos. Chem. Phys.*, 11, 9207-9218, 2011.

861 Wang, X., and Zhang M.: Vertical velocity in shallow convection for different plume types, J.
862 *Adv. Model. Earth Syst.*, 6, 478–489, 2014.

863 Wang, Y. and Geerts, B.: Composite Vertical Structure of Vertical Velocity in Nonprecipitating
864 Cumulus Clouds. *Mon. Wea. Rev.*, 141, 1673–1692, 2013.

865 Wang, Z. and co-authors: Single aircraft integration of remote sensing and in situ sampling for
866 the study of cloud microphysics and dynamics. *Bull. Amer. Meteor. Soc.*, 93, 653–668, 2012.

867 Weisman, M. L. and Klemp, J. B.: The dependence of numerically simulated convective storms
868 on vertical wind shear and buoyancy. *Monthly Weather Review*, 110, 504-520, 1982.

869 Wendisch, M., and Brenguier, J.: *Airborne Measurements for Environmental Research: Methods*
870 *and Instruments*. Wiley, 520 pages, 2013.

871 Wu, J., Del Genio, A. D., Yao, M.-S., and Wolf, A. B.: WRF and GISS SCM simulations of
872 convective updraft properties during TWP-ICE, *J. Geophys. Res.*, 114, D04206,
873 doi:10.1029/2008JD010851, 2009.

874 [Yang, J., Wang, Z., Heymsfield, A. J., and Luo, T.: Liquid/Ice Mass Partition in Tropical](#)
875 [Maritime Convective Clouds. *J. Atmos. Sci.*, in review, 2016.](#)

876 Zipser, E. J., Cecil, D. J., Liu, C., Nesbitt, S. W., and Yorty, D. P.: Where are the most intense
877 thunderstorms on Earth?. *Bull. Amer. Meteor. Soc.*, 87, 1057–1071, 2006.

878

Table 1. Number of penetrations, time in clouds and flight length in clouds sampled at 0–2 km, 2–4 km, 4–6 km, 6–8 km and 8–10 km MSL in HiCu, COPE and ICE-T.

Height (km MSL)	HiCu			COPE			ICE-T		
	Number of penetrations	Time in clouds (min)	Length in clouds (km)	Number of penetrations	Time in clouds (min)	Length in clouds (km)	Number of penetrations	Time in clouds (min)	Length in clouds (km)
8–10	43	12	79						
6–8	565	122	789				132	52	423
4–6	596	104	653	207	39	244	299	116	895
2–4	373	50	274	378	86	486	34	10	73
0–2				219	40	211	197	27	167

Table 2. Number of updrafts and downdrafts sampled at 0-2 km, 2-4 km, 4-6 km, 6-8 km and 8-10 km in HiCu, COPE and ICE-T.

Three numbers are given for the updraft and downdraft at each level, respectively, according to the three different definitions: weak, moderate and strong.

Height (km)		HiCu		COPE		ICE-T	
		Updraft	Downdraft	Updraft	Downdraft	Updraft	Downdraft
8-10	weak	66	100				
	moderate	52	44				
	strong	44	17				
6-8	weak	818	763			382	372
	moderate	559	540			175	136
	strong	287	130			102	23
4-6	weak	748	668	290	184	858	671
	moderate	522	389	232	193	425	329
	strong	343	48	135	51	266	73
2-4	weak	311	235	568	424	49	47
	moderate	271	84	467	434	51	51
	strong	149	7	188	101	32	10
0-2	weak			368	192	319	205
	moderate			266	90	234	104
	strong			96	9	60	7

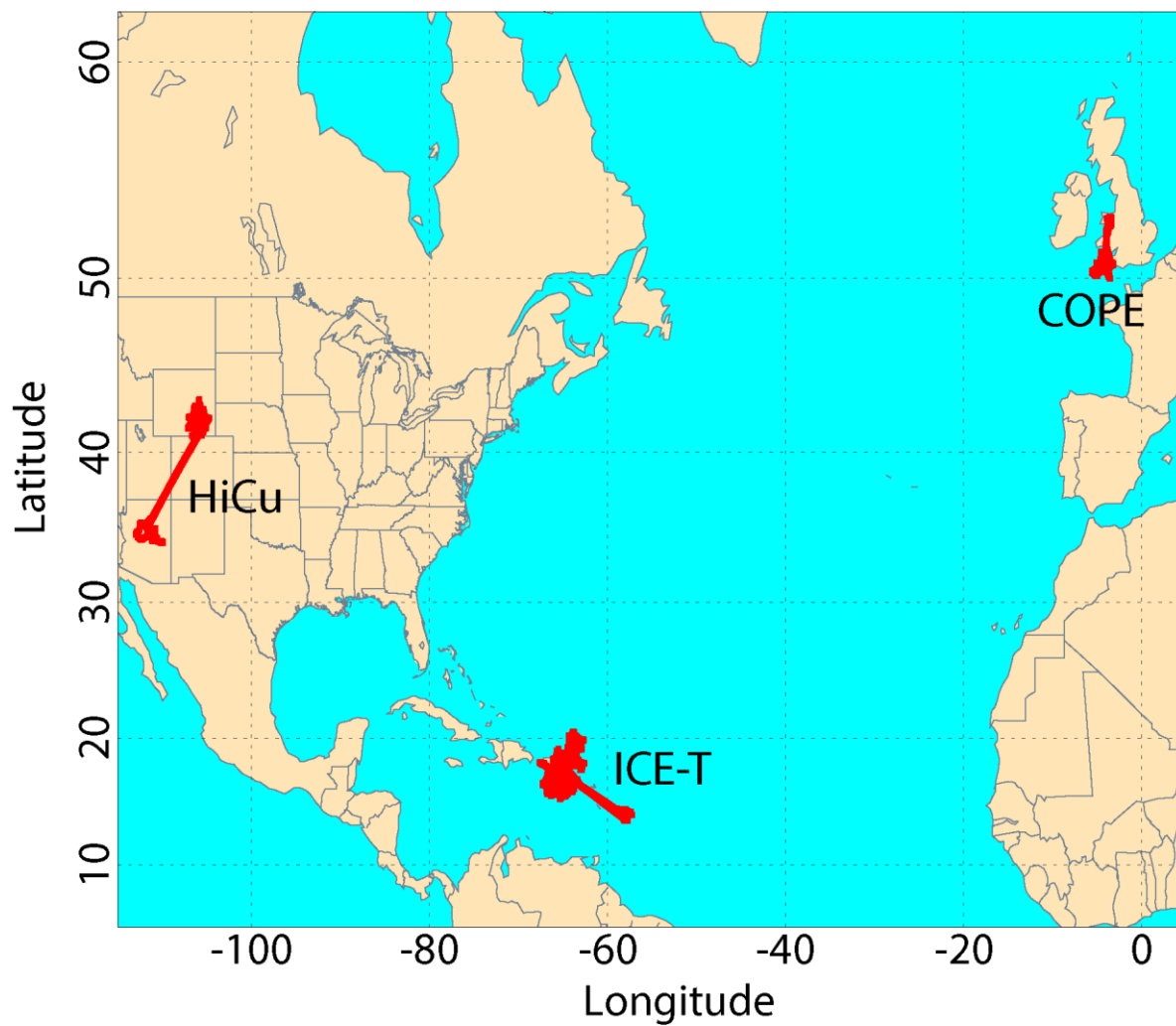


Figure 1. Flight tracks for the three field campaigns: HiCu, COPE and ICE-T.

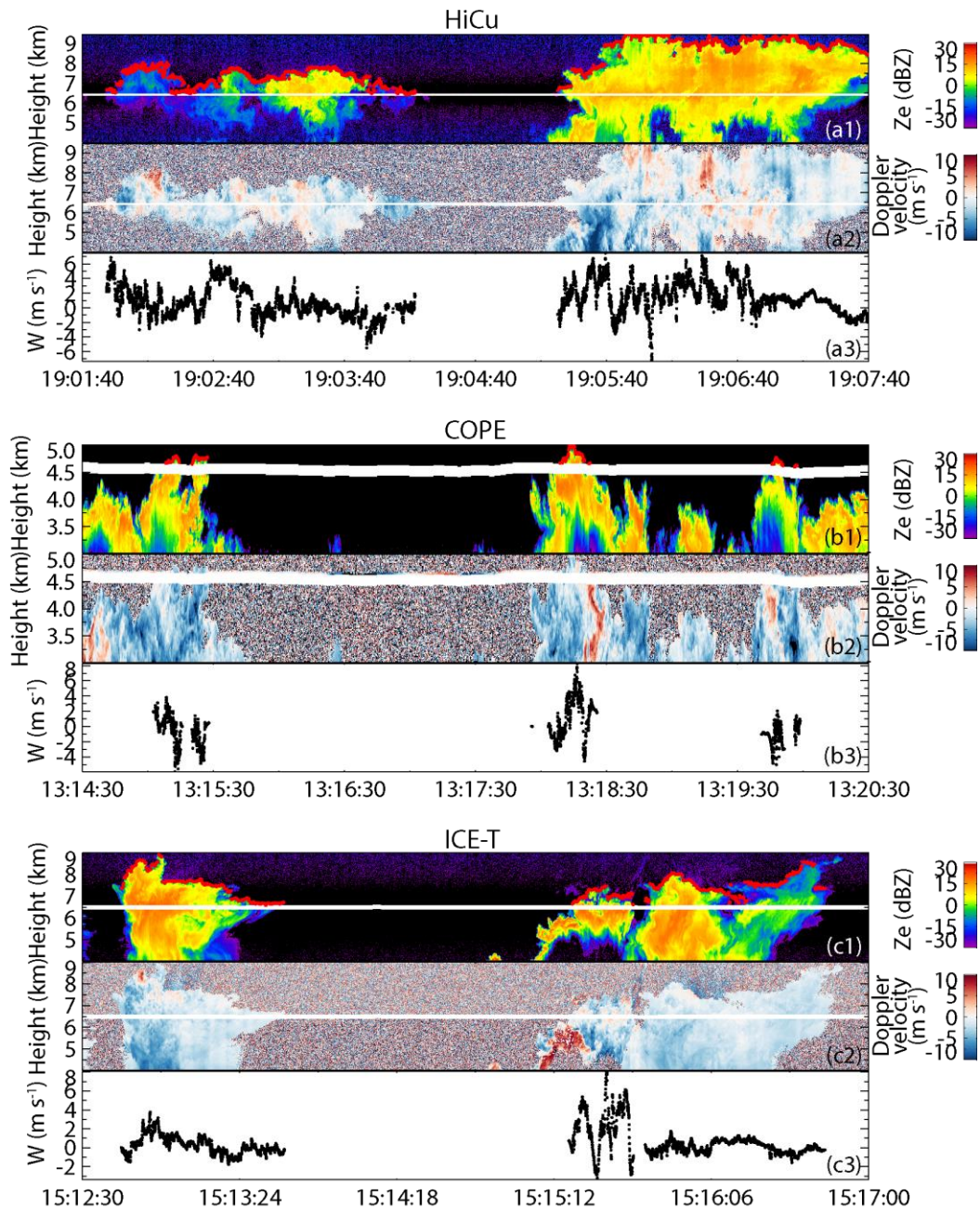


Figure 2. Examples of radar reflectivity, Doppler velocity and 25-Hz in-situ vertical velocity measurements for the convective clouds sampled in HiCu, COPE and ICE-T. The red dots in (a1), (b1) and (c1) are the cloud tops estimated by WCR.

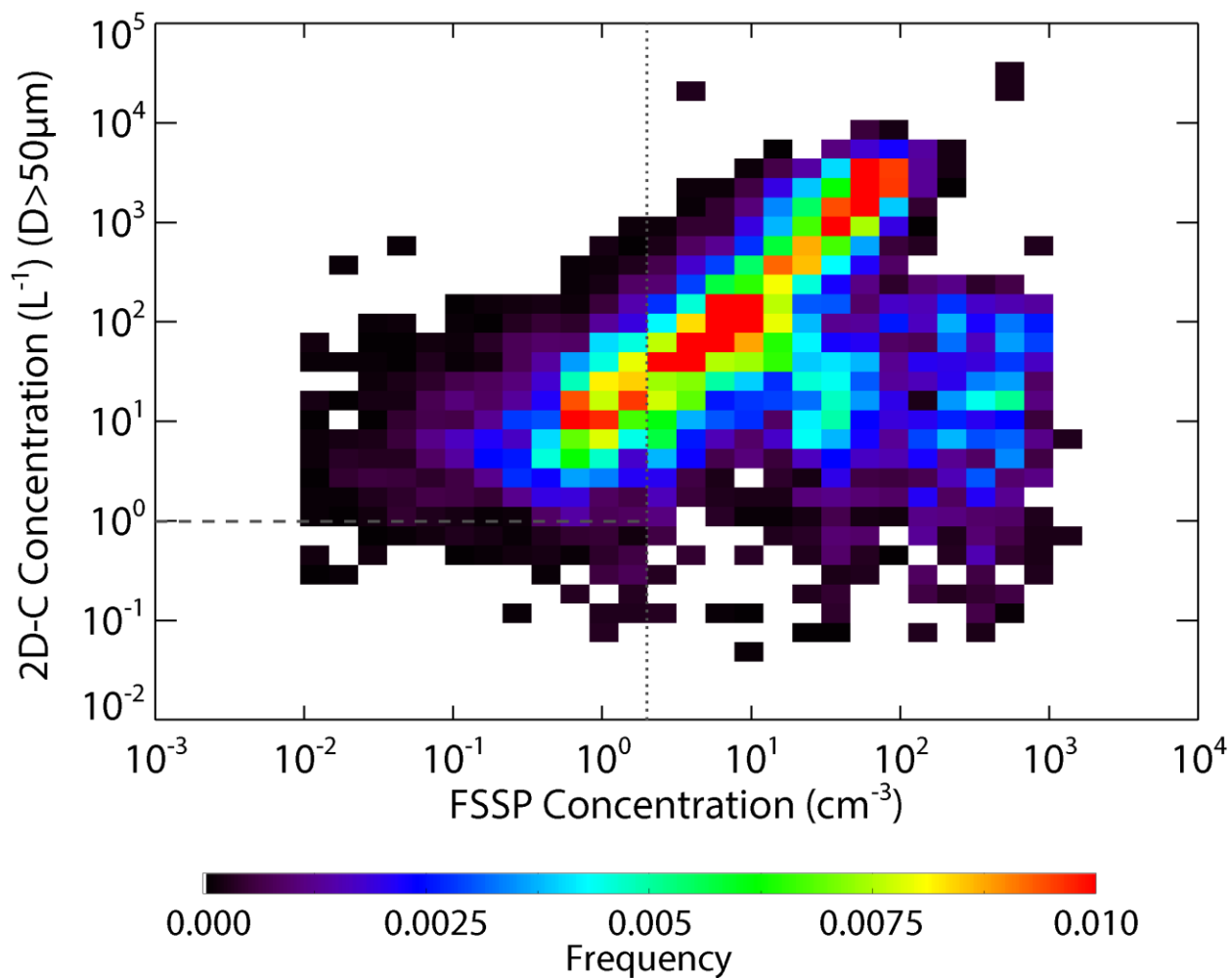


Figure 3. Occurrence distributions as a function of the particle concentrations measured by FSSP versus the concentrations of the particles $\geq 50 \mu\text{m}$ in diameter measured by 2D-C in the clouds identified by WCR reflectivity. The dashed and dotted lines indicate the FSSP concentration equal 2 cm^{-3} and the 2D-C concentration equal 1 L^{-1} , respectively.

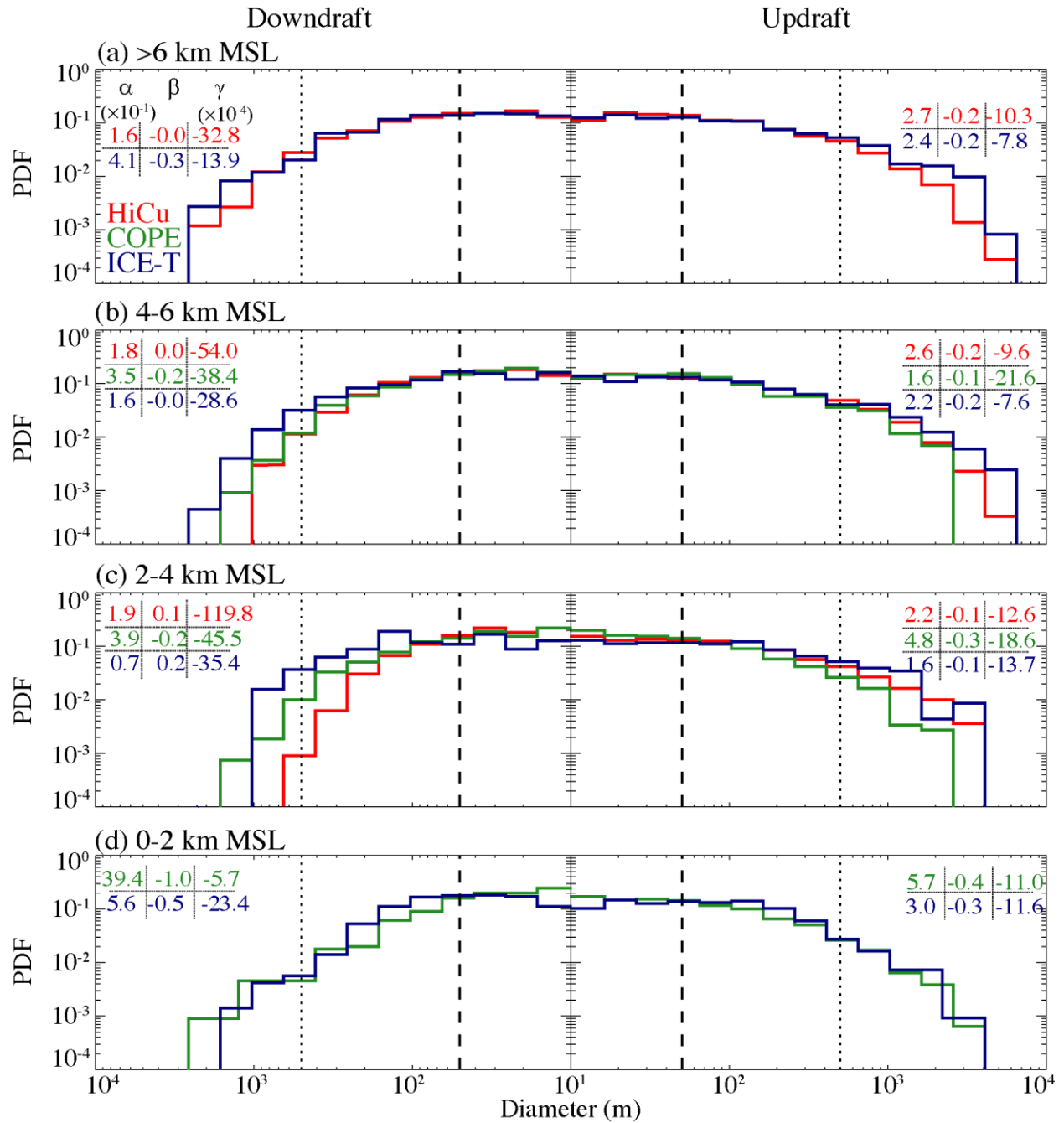


Figure 4. PDFs of the diameters for the updrafts and downdrafts sampled at 0–2 km, 2–4 km, 4–6 km and higher than 6 km. The numbers shown in each panel are the coefficients of the fitted exponential function (Eq. 1).

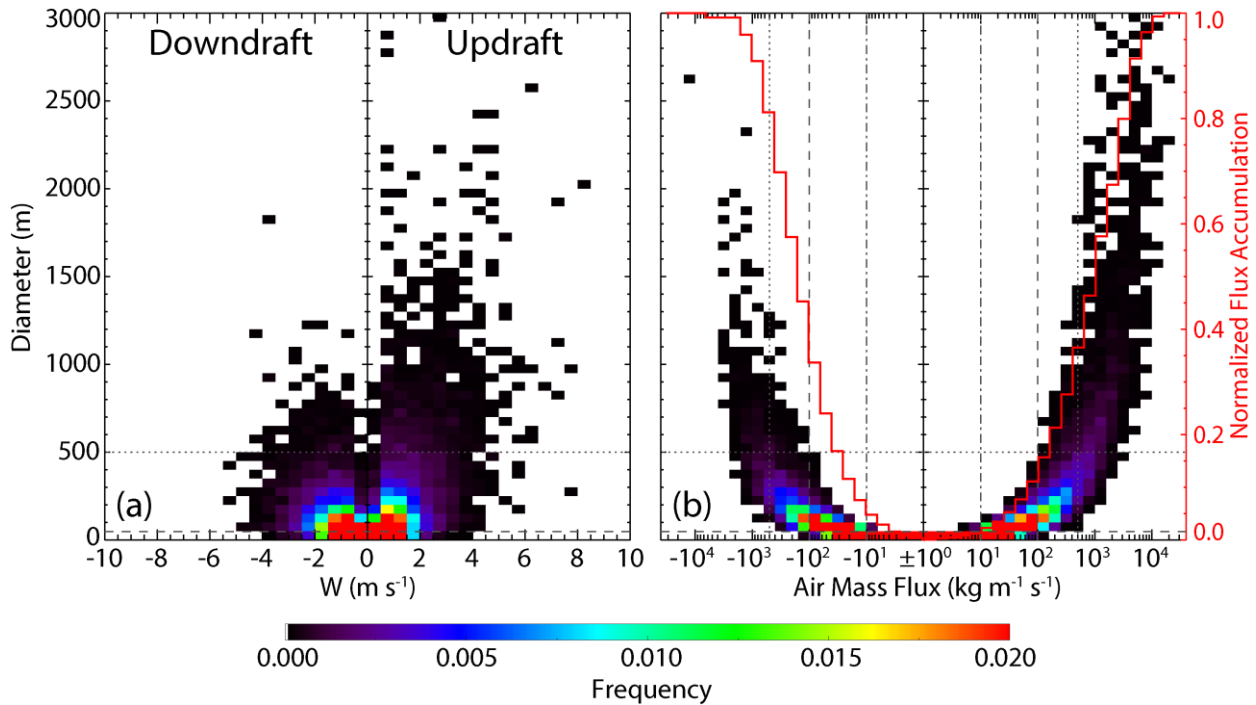


Figure 5. Occurrence distributions as (a) a function of diameter and mean vertical velocity, and (b) a function of diameter and air mass flux for all updrafts and downdrafts. The normalized accumulation flux is also shown by the red curves. The horizontal dotted and dashed lines in (a) and (b) indicate the draft diameter equal 500 m and 50 m, which are used as the diameter thresholds to identify a “draft” in previous studies and in this study, respectively. The vertical dash-dotted, dashed and dotted lines in (b) indicate air mass flux equal 10 kg m⁻¹ s⁻¹, 100 kg m⁻¹ s⁻¹ and 500 kg m⁻¹ s⁻¹ in magnitude, respectively, which are the thresholds used to delineate the three different groups of draft.

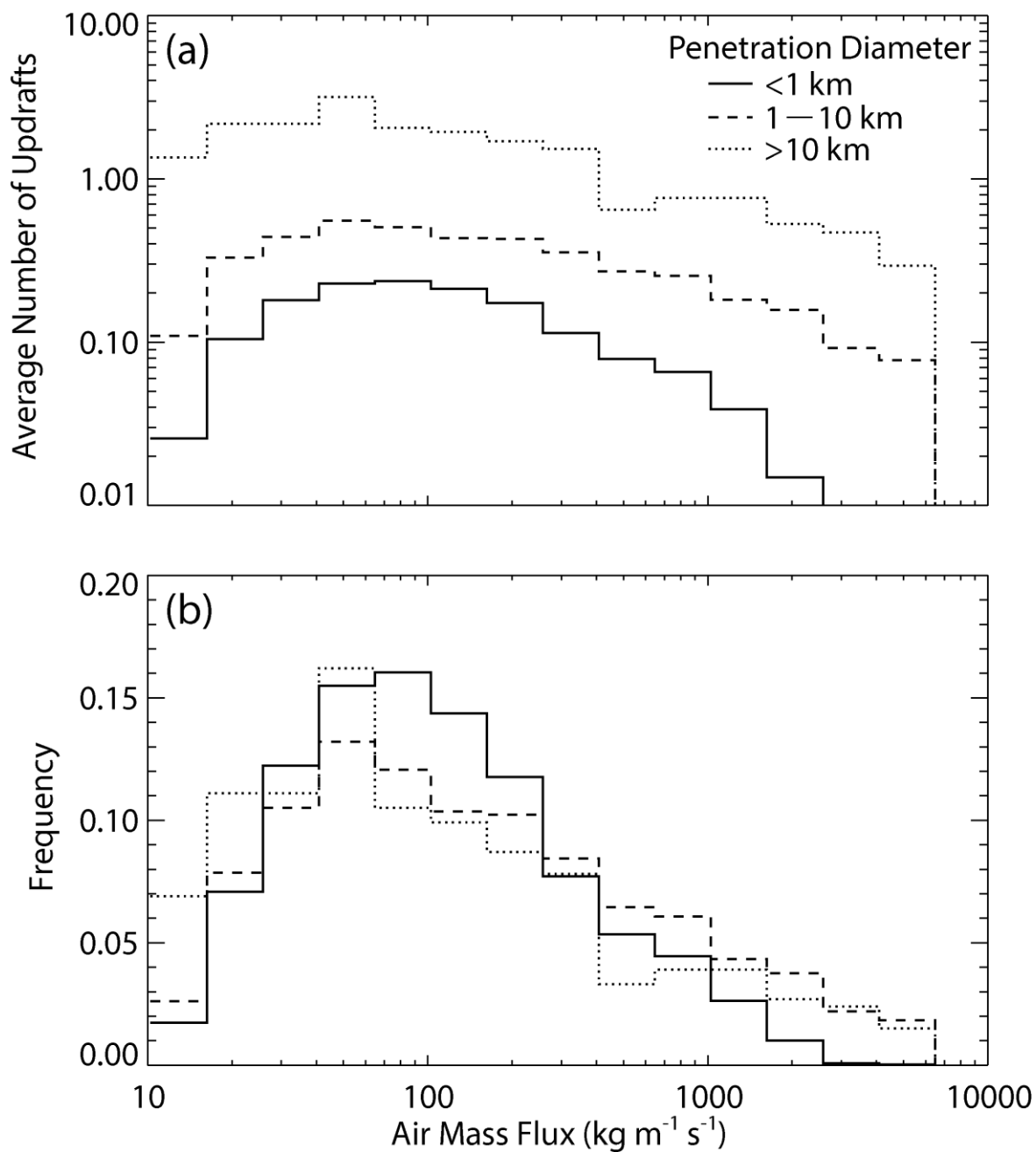


Figure 6. (a) Average number and (b) occurrence frequency of updrafts as a function of air mass flux observed in penetrations with length < 1 km (solid), 1-10 km (dashed) and >10 km (dotted). The result is a composite of HiCu, COPE and ICE-T.

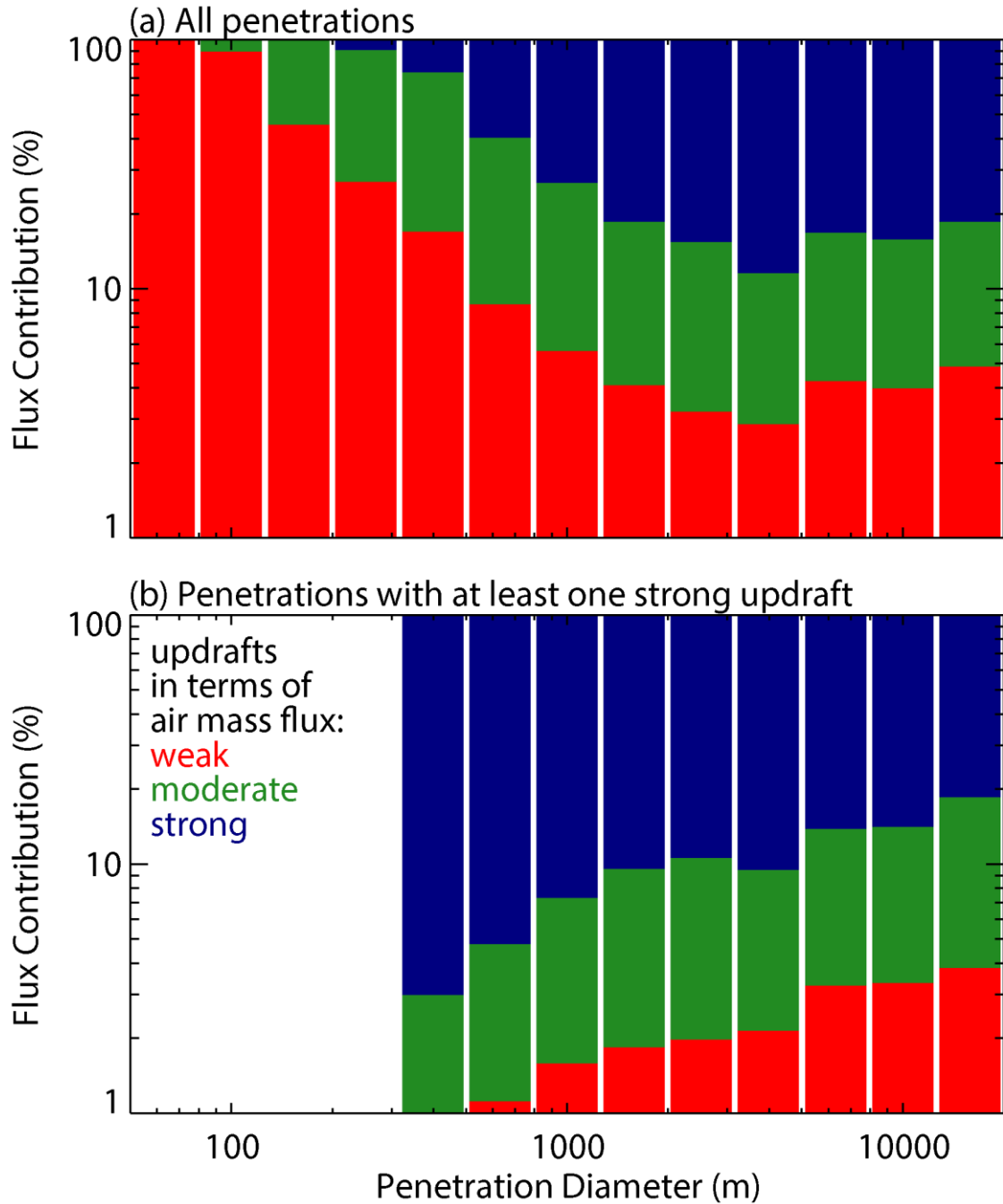


Figure 7. Average percentile contribution to total upward air mass flux by the weak (red), moderate (green) and strong (blue) updrafts delineated in this study. The result is a composite of HiCu, COPE and ICE-T.

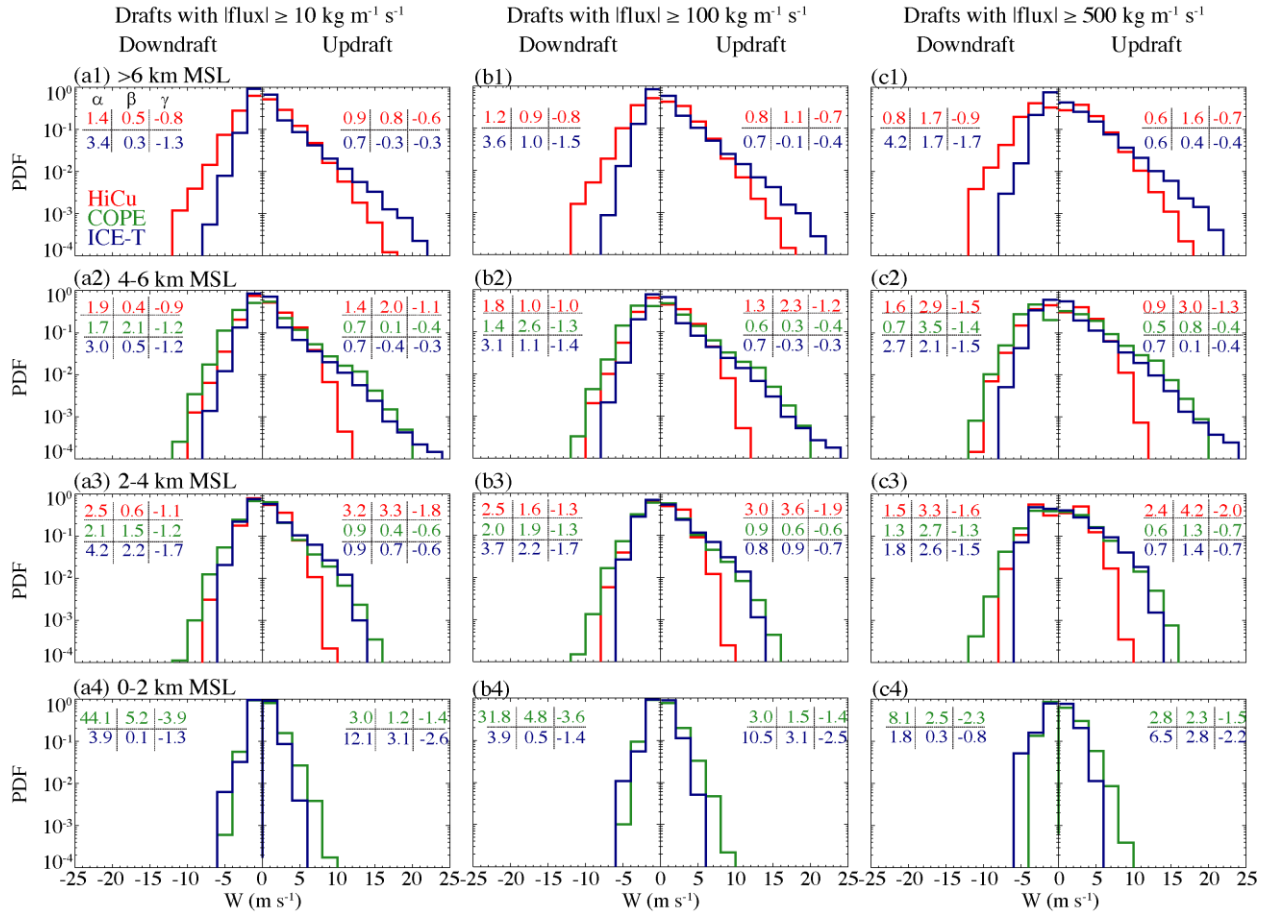


Figure 8. PDFs of the 25-Hz vertical velocity for the updrafts and downdrafts with air mass flux \geq (a) $10 \text{ kg m}^{-1} \text{ s}^{-1}$, (b) $100 \text{ kg m}^{-1} \text{ s}^{-1}$ and (c) $500 \text{ kg m}^{-1} \text{ s}^{-1}$ in magnitude, sampled at 0–2 km, 2–4 km, 4–6 km and higher than 6 km. The numbers shown in each panel are the coefficients of the fitted exponential function (Eq. 1).

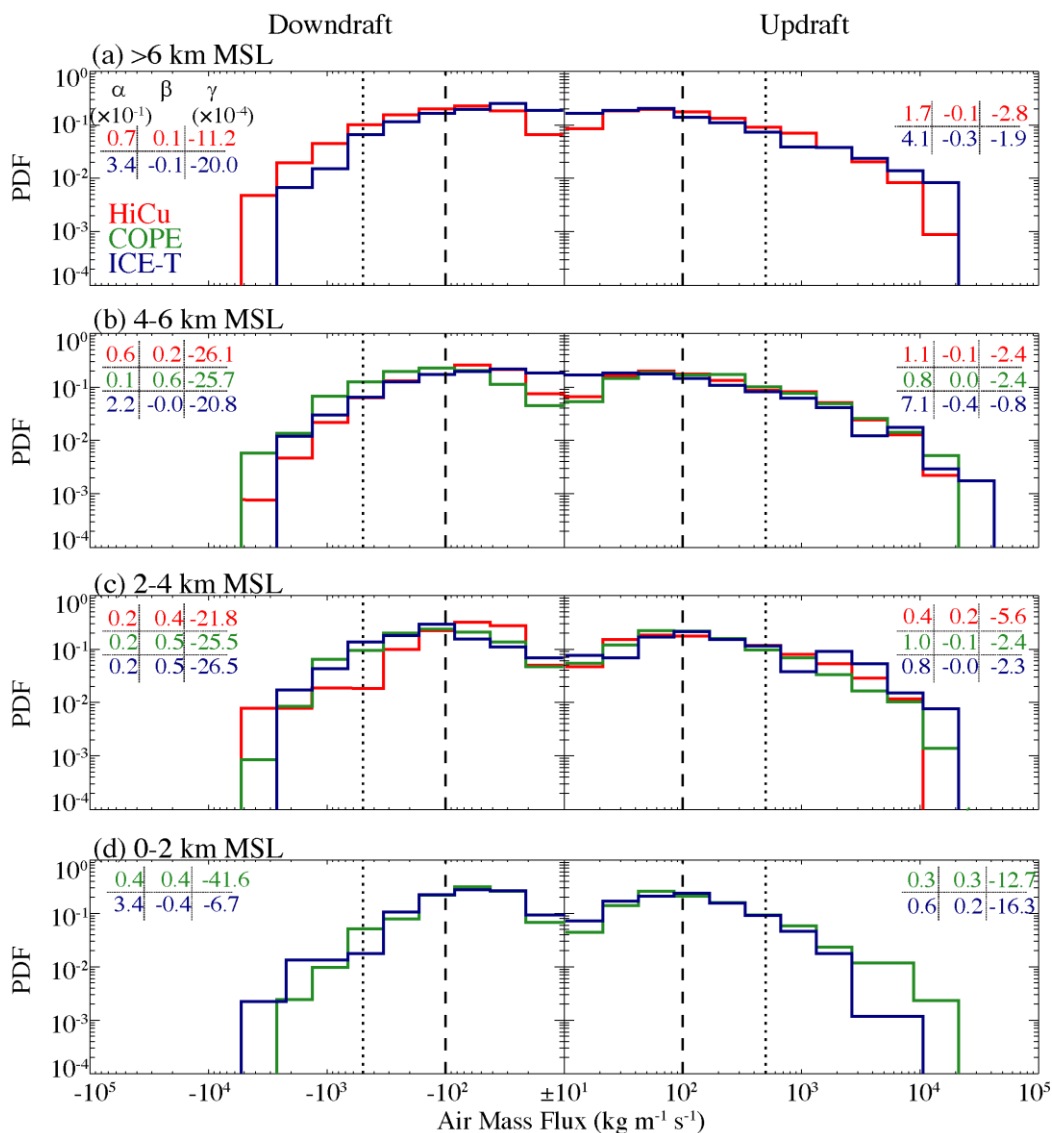


Figure 9. PDFs of the air mass flux for the updrafts and downdrafts sampled at 0–2 km, 2–4 km, 4–6 km and higher than 6 km. The three thresholds of the air mass flux ($\pm 10 \text{ kg m}^{-1} \text{ s}^{-1}$, $\pm 100 \text{ kg m}^{-1} \text{ s}^{-1}$ and $\pm 500 \text{ kg m}^{-1} \text{ s}^{-1}$) are shown by the solid (overlaps with the central y-axis in each panel), dashed and dotted lines. The numbers shown in each panel are the coefficients of the fitted exponential function (Eq. 1).

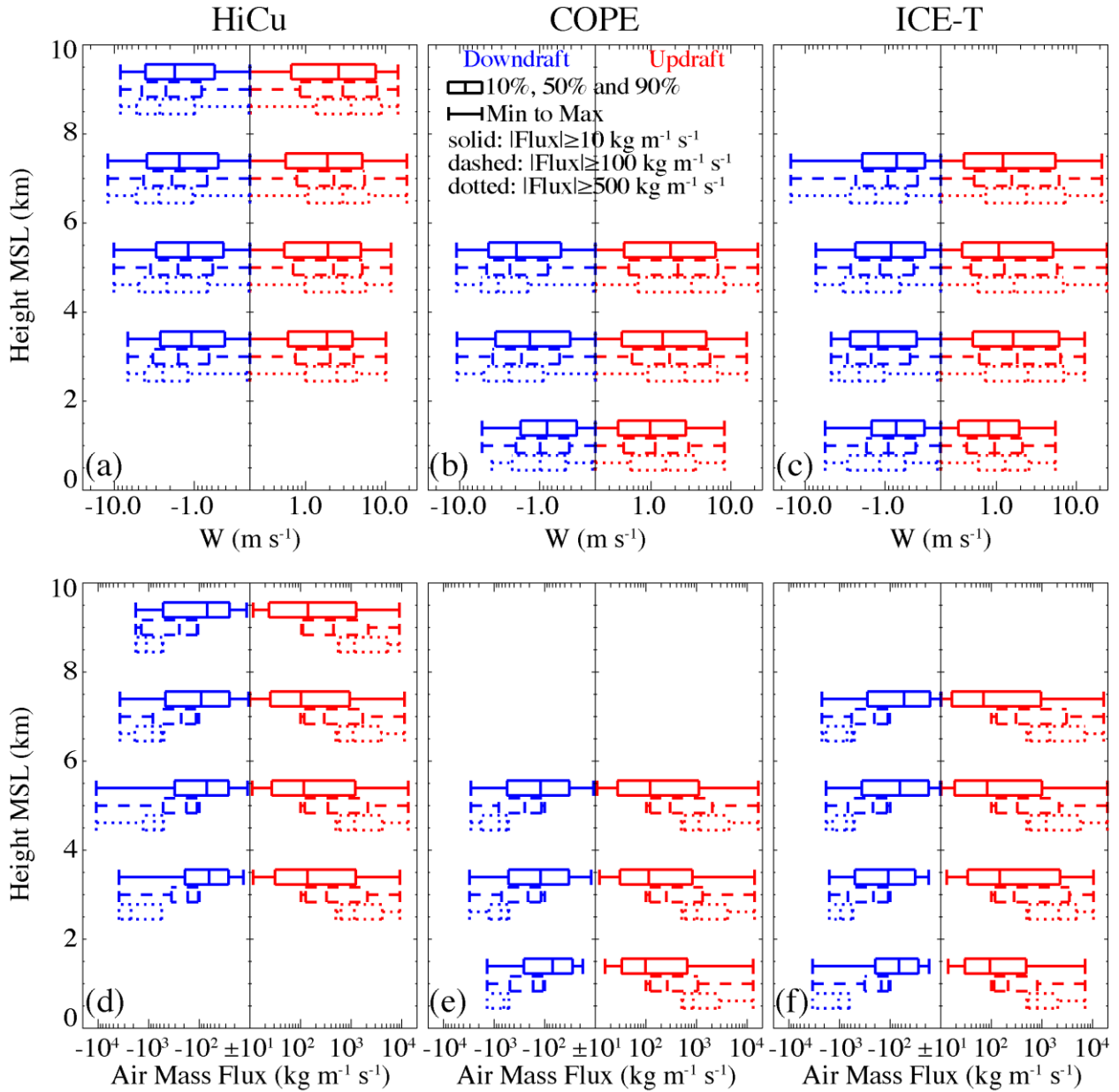


Figure 10. Profiles of (a-c) the vertical velocity and (d-f) air mass flux for all the updrafts and downdrafts sampled at 0–2 km, 2–4 km, 4–6 km, 6–8 km and 8–10 km. The dotted, dashed and solid boxes represent for the drafts with air mass flux $\geq 10 \text{ kg m}^{-1} \text{ s}^{-1}$, $100 \text{ kg m}^{-1} \text{ s}^{-1}$ and $500 \text{ kg m}^{-1} \text{ s}^{-1}$ in magnitude, respectively.

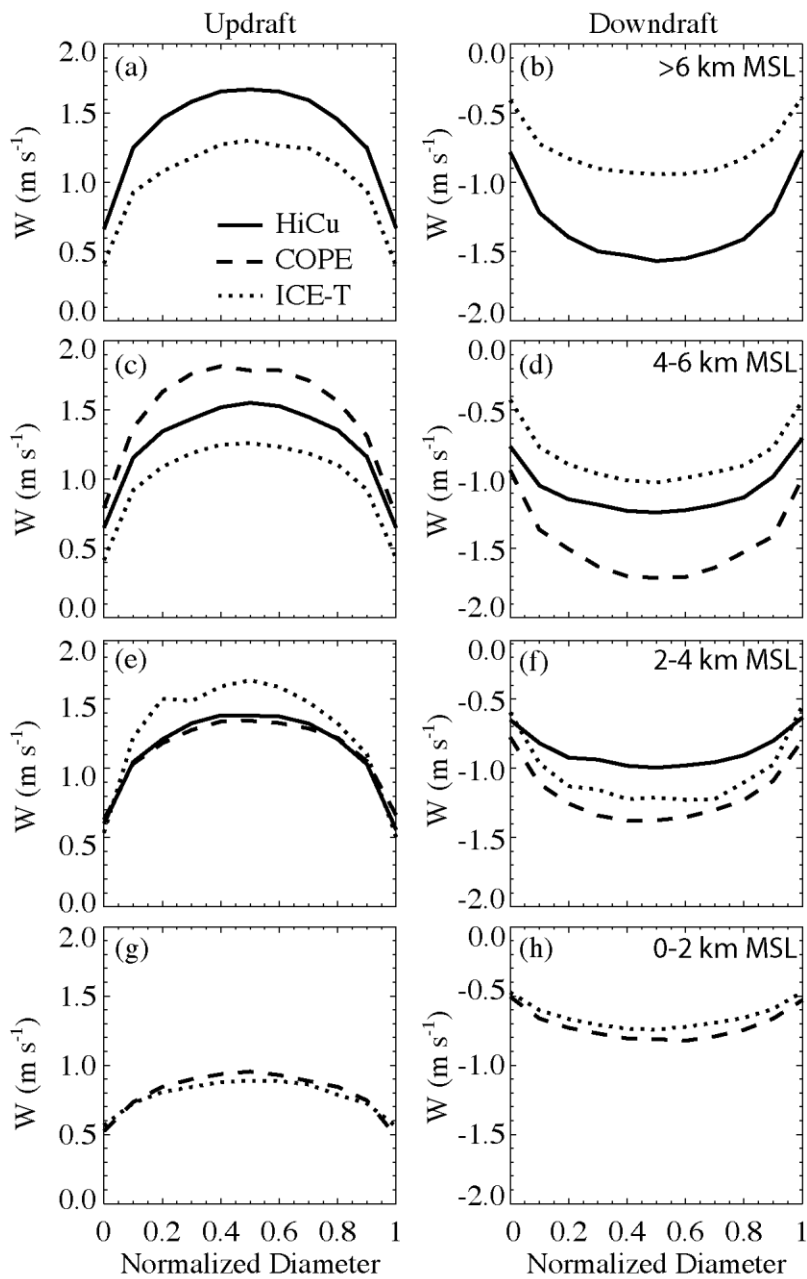


Figure 11. Composite structure of the vertical velocity as a function of the normalized diameter for the updrafts and downdrafts with air mass flux $\geq 10 \text{ kg m}^{-1} \text{ s}^{-1}$ in magnitude. The 0 and 1 coordinates on the x-axis indicate the upwind and downwind sides of the draft.

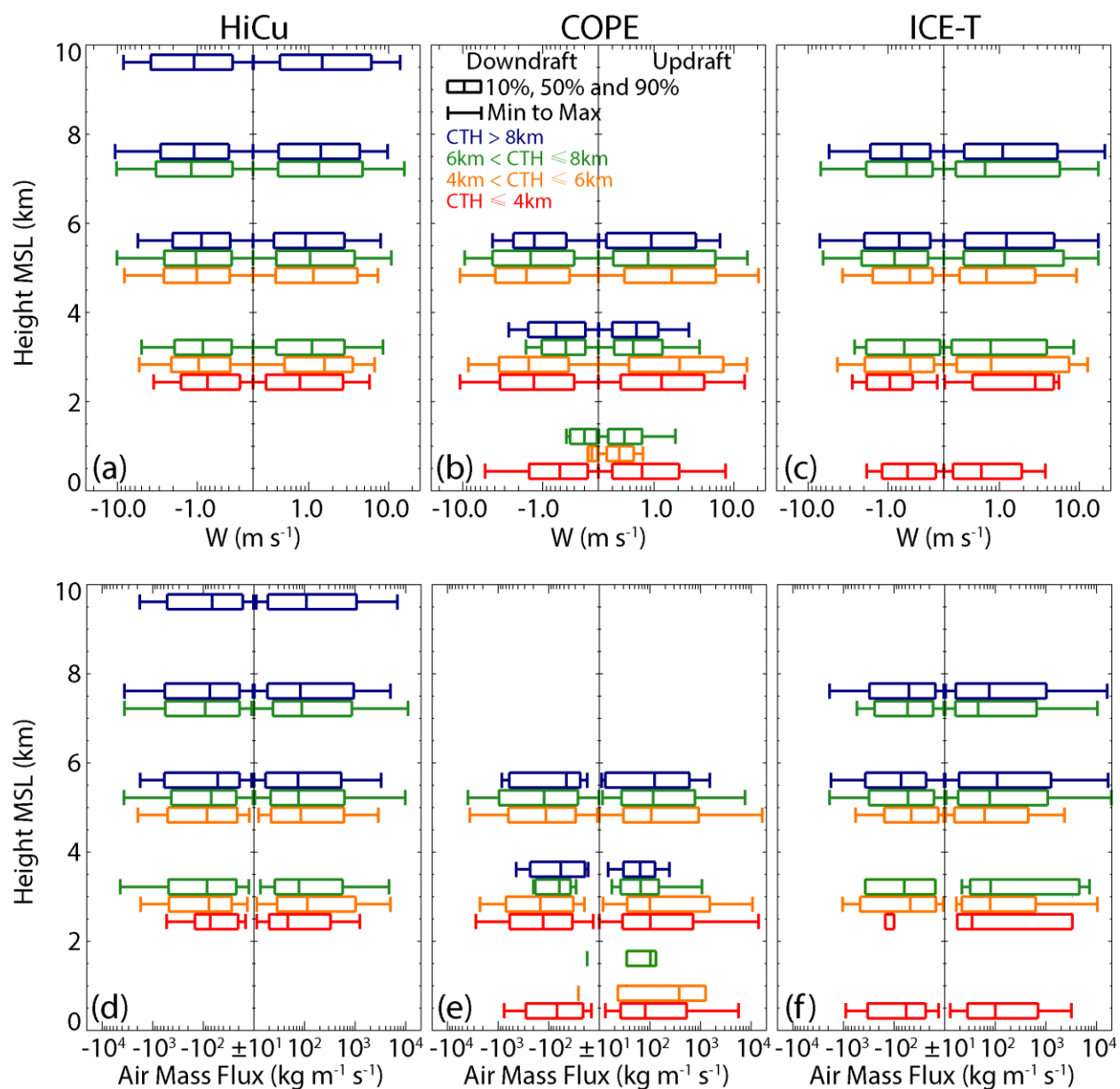


Figure 12. Profiles of (a-c) the vertical velocity and (d-f) the air mass flux for the updraft and downdraft with air mass flux $\geq 10 \text{ kg m}^{-1} \text{ s}^{-1}$ in magnitude. The red, orange, green and blue boxes represent clouds with cloud top heights of 0-4 km, 4-6 km, 6-8 km and higher than 8 km.